A Comprehensive Toolset for Signal Processing using a Family of Hadamard Transforms

Dure Jabeen[1], Tahmina Khan[2], S. M. Ghazanfar Monir[3], Dilbar Hussain[1], Rumaisa Iftikhar[4]
[1]Department of Computer Science, Main Campus, IQRA University, Karachi.
[2]Department of Computer Information Technology, Aligarh Institute of Technology (AIT).
[3]Karachi School of Business & Leadership.
[4]Department of Electronic Engineering, Sir Syed University of Engineering and Technology, Karachi.
*** Correspondence.** Dure Jabeen and Email. durejabeen@hotmail.com.

Citation | Jabeen D. Khan. T, Monir. S. M. G., Hussain. D, Iftikhar. R, "A Comprehensive Toolset for Signal Processing using Family of Hadamard Transforms", IJIST, Vol. 07, Issue. 02 pp 770-801, May 2025
Received | April 15, 2025 **Revised |** May 10, 2025 **Accepted |** May 13, 2025 **Published |** May 14, 2025.

Independent basis of the linear vectors is of paramount significance in the advancement of digital systems that facilitate the processing and storage of information in its digital format. This study undertakes a thorough examination of discrete orthogonal transformations, with particular focus on the family of real and complex Hadamard transforms and their numerous types. The efficacy of various sequences is scrutinized, alongside their mathematical representation, inherent characteristics, and applications in signal processing. An analysis of the computational cost associated with the complex Hadamard Transform and its variants is presented. Furthermore, simulation outcomes are contrasted for the normalized sequency concerning magnitude response, image compression, and peak signal-to-noise ratio across a variety of image processing applications.

Keywords. Basis Vectors, Signal Processing, Real and Complex Signals, Sequency Domain.

Introduction.

Over the last ten years, the utilization of Discrete Orthogonal Transformations (DOT) in digital signal and image processing has gained substantial grip. Its considerable impact on high-performance digital computer systems, the notable developments in digital technology, and the emergence of specialized digital processors as a result are all factors contributing to this growing interest. The general field of data processing has benefited greatly from the widespread use of minicomputers, microprocessors, and mini/microsystems. Fast methods based on matrix factorization, segmentation, and other techniques [1][2][3][4][5] have reduced computational and memory requirements while making these transformations more effective and applicable. Another benefit of these algorithms is their reduced round-off error [6][7]. Consequently, there has been a push to establish and standardize notation and nomenclature for orthogonal functions and digital processing.

Examination and exploration of the various associated fields and their applications of DOTs which may comprise image processing [8][9][10][11][12][13][14][15][16][17][18], selection of features under the pattern recognition analysis [19][20][21][22], character identification [23][24], verification of signature[25][26][27], binary sequences depiction, examination of various systems of communication [28][29][30][31][32][33][34], digital systems [35][36][37][38][39][40][41], analysis of signals in frequency domain [4][42][43][44][45], information compression [46][47][48][49], signal analysis and synthesis [50][51][52][53], understanding the characteristic of the systems and degree of similarity of systems [54][55][56][57], widespread Wiener filtering [58][59][60], spectrometric imaging [61][62], systems analysis [63][64][65], identify the information [66][67], stochastic examination [68][69][70], study of spectrum [71][72] and other areas. Orthogonal transforms (OTs) are linear combinations of the row vectors of their respective transformation matrices. For instance, OTs have been practiced for different datasets such as linear, non-linear signals, voice, earthquake, sound navigation and ranging signals, bio-logical, bio-medical, astronomical signals, satellite imaging, aerial reconnaissance, images data for disasters like (flood, rain, weather, etc.), CCTV images, sensor-based data, electron micrographs, range-Doppler planes, thermograms, X-rays, EEG, ECG, two-dimensional images of the human structure of the body, pandemic, natural disaster data, etc. As a result, the wide scope of multidisciplinary research in this field is evident. The existence of material dedicated exclusively to these topics highlights the growing importance of rapidly applying digital technologies and processing techniques.

Image processing techniques include spatial filtering, image coding, image restoration and enhancement, color and grey imagery, image data extraction and detection, image diagnosis, machine learning, deep learning, Wiener filtering, feature selection, pattern recognition, digital holography, digital and analogue filtering, Kalman filtering, and industrial testing. For image improvement and restoration, data detection/extraction, image classification, and other artificial intelligence applications, the transform domain of the grey image and color-coding has been used. The converted data's high-energy compaction feature helps to minimize data rate needs (decrease similar information), make significant changes in channel error acceptance, and achieve sample and/or bit reduction.

In many circumstances, image processing using computer techniques such as big data necessitates the use of DOTs are classified as either optimal (Karhunen Loeve Transform) or suboptimal (Karhunen Loeve Transform) [73][74]. The second group is further subdivided into two groups (I and II). DFT, CHT, and their variants are examples of transformations whose basis functions are on the circle with unit values. All other transforms are classified as category II, which is further separated into sinusoidal and non-sinusoidal varieties as shown in Figure 1.

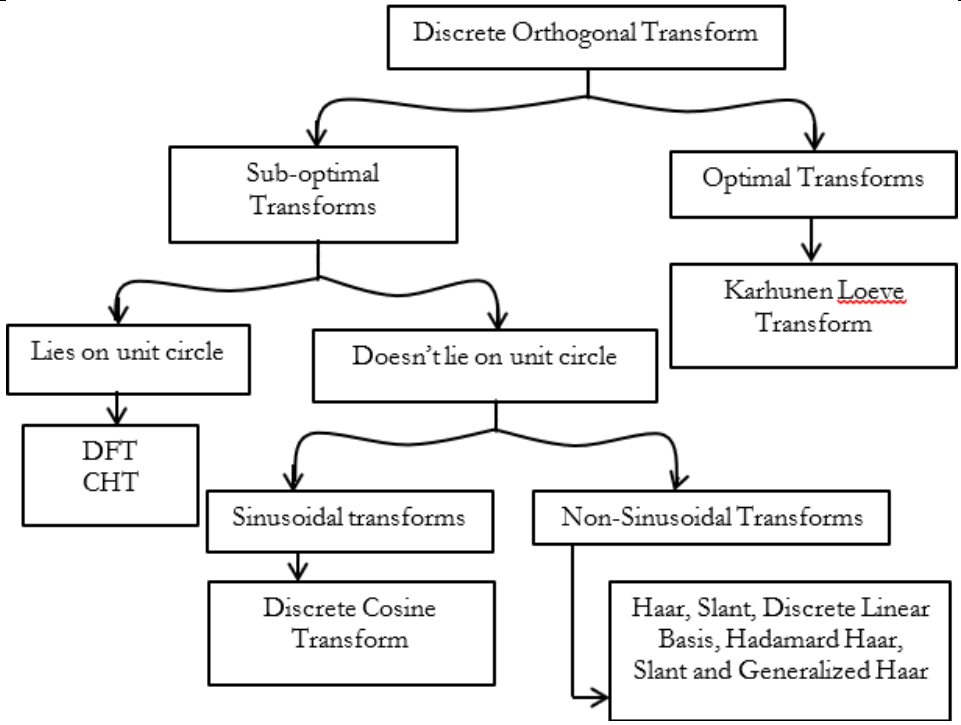

Figure 1. The orthogonal transforms based on kernel function characteristics.

This paper focuses on both real and complex Hadamard transforms and their various forms. The Walsh-Hadamard Transform (WHT) [75], a type of real Hadamard transform, is capable of representing square or rectangular waveforms. Its various forms are suited to different applications; for instance, the sequency-ordered version is well-suited for communication systems, while the signal processing variant is more appropriate for tasks such as spectral analysis and filtering [76][77]. In (2009) [78], A. Aung proposed the properties of the Complex Hadamard transform (CHT). Some variants have a sequency property that is like the DFT based on the unit circle. Complex Hadamard Transform is the modified version of the real Hadamard transform, and its variants are. 1) Sequency Ordered Complex Hadamard transform (SCHT) [79], Natural Ordered Complex Hadamard Transform (NCHT) [80], and Conjugate Symmetry Sequency Ordered Complex Hadamard transform (CS-SCHT) [81]. The Walsh-Hadamard transform family is shown in Figure 2. The fundamental functionalities of the (DOTs) are discussed, along with image de-noising and compression techniques specific to the CHT variants.

The main objective of this research endeavor is to assess the computational expenditure associated with the complex Hadamard Transform and its various types. Furthermore, it examines the simulation outcomes that concentrate on normalized sequency, scrutinizing performance metrics concerning magnitude response, image compression efficacy, and peak signal-to-noise ratio across a range of image processing contexts. The originality of this investigation resides in its comprehensive comparative analysis of complex Hadamard Transform variants through an exhaustive evaluation of computational costs, alongside application-oriented simulations. By integrating normalized sequency as a pivotal metric across an array of image processing applications, this research provides unique perspectives on the performance characteristics of the transform, especially concerning the interplay between image quality and compression parameters.

This work is divided into five sections. Section I is an introduction, Section II is a detailed analysis of real and complex Hadamard transform variants, and Section III is a detailed investigation of real and complex Hadamard transform variants. In section IV, the simulation findings are examined, and in section V, the conclusion is offered.

Walsh-Hadamard Transform and Its Applications.

The Walsh-Hadamard transform is a generalized variant of the Fourier transform and is also known as the Walsh function, Hadamard transform, Rademacher function, and Walsh-Fourier function.

Real Hadamard Transform.

The Hadamard Transform is well-known for its simplicity and straightforward transformation matrix. The Real Hadamard Transform is commonly represented using Walsh basis functions; square or rectangular waveforms characterized by alternating values within the matrix; collectively referred to as WHT [74][82]. The row vectors of the WHT matrix can be interchanged while preserving the orthogonality to obtain different orderings of the WHT [75]. Conventionally used orderings are Walsh or Sequency order, Hadamard order, and Dyadic or Paley order. Each ordering has different applications in signal processing and digital communications systems. The basis function of all real orderings is defined in [75] are discussed in the following section. The different orderings of the WHT are illustrated in Figure 2 and are described in detail below.

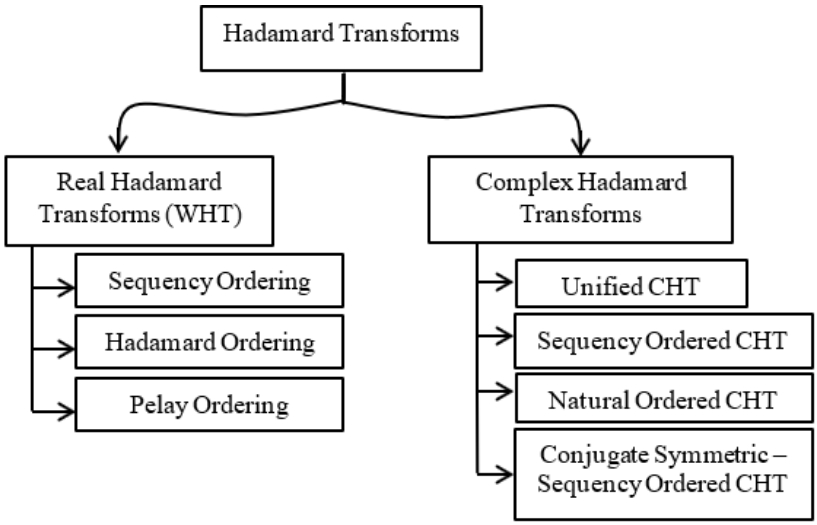

Figure 2. Taxonomy of Hadamard transforms based on their variants.

Natural/Hadamard Ordering.

This ordering is derived from the recursive application of the Kronecker product on the right-hand side. It results in what is known as natural ordering, where the sequence, defined as the number of sign changes in each row vector of the transformation matrix, follows a specific pattern generated by this recursive structure. Hadamard matrices are of order and are generated as,

$$\mathbf{B}_N = \mathbf{B}_2 \otimes \mathbf{B}_{N/2} \quad (1)$$

Where B_N It is a Hadamard matrix, $\otimes$ Kronecker product operator [74]. Hadamard sequences are used in several applications [83].

Dyadic/Pelay Ordering.

This type of ordering can be generated by the bit-reversed order of the Natural/Hadamard ordering [75].

Walsh/Sequency Ordering.

The construction of the Walsh ordering depends on the Rademacher function (RADM); it is a series of orthogonal rectangular pulses with $\langle \pm \rangle$ Values. The RAD function can be represented as,

$$RADM(l,t) = sign\left(sin\left(2^l \pi t\right)\right) \quad (2)$$

RADM function has two arguments *l* and *t, l* represents the discrete samples, which are equally spaced over a normalized time base $t \in [0,1)$, $l = 2^n$, $n = log2(N)$ and *t* vary from [0.1, 0.2, 0.3…1]. RAD function depends on the hard limiting signum with its argument in radians [74].

WHT Properties.

Discrete Fourier Transform (DFT) and Walsh Hadamard Transform (WHT) exhibit several similar properties, as noted in [84]. Nomenclature of WHT basis functions has been introduced with sequency, Sine Walsh and Cosine Walsh sets, where it has been observed that dyadic convolution and dyadic correlation are identical due to modulo-2 operation (addition/subtraction). Q-spectrum is known for the WHT circular shift-invariant; it is invariant to the cyclic shift of the DFT with the shift-invariant power spectrum [85][86]. WHT dyadic shift property and shift invariant power spectrum have been derived by the H-diagram [87]. To uncover new permutation groups, the input pattern power spectrum of WHT has been studied utilizing various transformations, such as moving patterns cyclically and multiplying by 900 rotation with the input signals [88]. In [89], WHT vector integers possessed the even or odd coefficient property by which data was compressed in a quantized way. In [90] S. Barentt, he commented [89] that the matrices he has presented have even or zero value by the same parity of a_i and the input vector x_j. Although; h_ij matrix has odd integers with positive and negative elements. Using their intrinsic reporters, WHT and Discrete Cosine Transform (DCT) were used to generate a direct matrix transformation in [91]. WHT multi-polarity properties have been introduced for the area of logic design by B. J. Falkowski [92]. For the mathematical applications [93][94][95], WHT properties like the reverse jacket matrices (RJM) and Restclass RJM have been derived, whereas WHT is a special case of RJM. With similar features and a lower computing cost than DFT, the Sequency Generalized Walsh Hadamard Transform (SGWHT) [96] has been created. The SGWHT has specific cases known as WHT, SCHT, and DFT.

WHT Implementation.

Walsh-Hadamard transform has been implemented as a finite set of Walsh functions [97] and Discrete Walsh functions [98], using the Kronecker product [99] and WHT matrices, with the help of linear feedback, shift registers [100][101]a. In the 1970s, WHT got popular in image/signal processing applications due to its simplicity and inherent efficiency of implementation [97] that was comparable to the Cooley-Tukey algorithm [75]. WHT is diagonally structured and implemented, computing the DCT on real-time image processors [102][103]. A 16-point binDCT has been implemented covering the gap between DFT and WHT for the lossless compression and precision in the floating-point DCT [104], while DCT is implemented with WHT for a high-level video coding scheme [105]. Fast WHT (FWHT) has been implemented for three-phase systems. When the fault occurred in the symmetrical system components, the filtered output of the three-phase sequence was calculated by using FWHT [106]. DFT-WHT has been implemented using the sparse matrix concept with the single butterfly structure [107], and the Walsh spectral coefficients have been represented by the Boolean functions with formation and generations as multi-polarity of WHT [92]. In [108], a novel realization scheme and adaptive filters [76][109][110] have been presented for the two-dimensional digital filters using the discrete structure with noise characteristics. The least mean square (LMS) adaptive filters have been implemented using WHT, which increases the speed of the filters [111]. The isotropic filter is proposed in [112][113] using WHT with increased convergence rate of the filter and reduced computational complexity of the quadratic filters. For better performance and design approach, WHT has been implemented using VLSI [114], and a uniform comprehensive approach of reverse jacket transform has been introduced that unifies the Walsh transforms in it [115].

Fast WHT has been collectively used with DFT as a single transform for the OFDM system in [116]; it is used to reduce the computational complexity and Peak to Average Power Ratio (PAPR) [117][118]. In [119], the proposed method improves Peak to Average Power Ratio (PAPR) by using linear pre-coding with WHT. By combining the mentioned name of transforms, 36% to 70% of the hardware runtime is reduced [120]. Regardless of the size of the basis vectors, WHT has been implemented as a recursive method for the sliding window in [121]. To enhance performance and reduce residual complexity, an automated scheme based on Discrete Orthogonal Transforms (DOTs) has been implemented for the modeling and optimization of various signal transformations [122][123][124]. FFT and WHT are integrated to increase the efficiency of large-signal transformations in terms of their dynamic layout and use of cache capacity [125]. The Haar wavelet transform (WHT) has appealing characteristics and parallelization features [126]. Based on the R-radix factorization matrices, which were perfect iterative systems with fewer memory shift registers, a family of identical sparse matrices has been developed in [127].

WHT in Digital Communication.

The antipodal information with WH matrices was used to show the Rayleigh fading channel coded modulation technique [128]. Utilizing WHT at lower power levels and compressive sensing applications with a slow ADC sampling rate, ultra-wideband is implemented [129]. Projection-based results reveal that the single-shot transmission and GFDM-WHT technique produce superior outcomes than the conventional GFDM for the 5G network. This approach was proposed to be robust against the frequency-selective channels employing GFDM and WHT [130].

What is Image Processing?

It has been observed in the literature review that WHT has been applied to block-wise processing, feature selection, image sensing, and image and data compression [131][46][132][133]. Unified lossless WHT (ULWHT) has been created for lossless data compression applications in [134][135]. After applying the proposed transform to the collective image coefficients or blocks, the entropy initially decreased, indicating improved compression efficiency, but began to increase again as the block size became larger. It performed better for the small-sized matrix for the lossless data using the ULWHT. In [136], block-wise WHT was introduced for the illumination variations of the face reorganization. The suggested solution outperformed the Discrete Cosine Transform (DCT) in both cases of higher illumination and lower illumination with reduced computing expense. Through picture pattern recognition of the multilayered neural networks, an image that was produced by an invariant step is recognized [137]. Based on the Human Visual System (HVS), image watermarking techniques were proposed using WHT in [138]. The host and watermarked image both contained the coefficient of the watermarked key. Compared to other DOTs, a WHT method has greater robustness against various attacks. The Haar Discrete Wavelet Transform (HDWT) performs worse than WHT and DCT, according to optical image watermarking algorithms in [139]. By utilizing sub-pixel-speckle shifting in ghost photography, low-resolution imaging can be enhanced to improve edge detection capabilities, allowing for finer structural details to be captured more effectively [140].

WHT in Signal Processing.

The understandable voice data was recreated in the non-real-time mod in [141] utilizing the dominating coefficients of the Hadamard and Walsh transforms. The degradation in the reconstruction was removed by moving the sampling window on the spectra [142] on the stochastic system with dyadic symmetry using WHT for the statistical analysis. The WHT has proven to be effective for exploiting the convolution property. Additionally, it is well-suited for processing statistical data in the transform domain due to its shared characteristics with the Fourier Transform. The shift-invariant characteristic of the particular case of WHT,

dyadic shift employing dyadic ordering [87], was used to generate the power spectrum. For the stationary process for DOTs, it has been proposed to efficiently pack the energy in the m-coefficients of the transforms [143]. For the set of invariant transformations, modified-WHT was used in the literature review, and it converged all mapping qualities at a single point [144]. In general, real transforms are employed for real input signals, although some signals are in-phase and quadrature in nature in the digital signal processing domain. As a result, the real Hadamard Transform was introduced for complex input signals in [145], and the resulting spectra had Fourier-like features with fewer calculations due to its transformation matrix values. WHT aided in computing the k-sparse WHT for the N-dimensional signals [124]. WHT was first used in video compression coding schemes in [146], and it matched multilayer blocks diagonally while rejecting some starting blocks. It performs better for clock-matched motion estimation without the cost of PAPR.

In [147], WHT is also introduced for Boolean functions.

Complex Hadamard Transform and Its Applications.

The CHT family is depicted in Figure 3. A limitation of the Real Hadamard Transform is that it operates exclusively on real-valued functions. However, it offers computational simplicity, requiring only additions and subtractions for its implementation. CHT, also known as complex BIFORE (binary Fourier representation) transforms (CBT), have been explored in the literature [148]. It deals with complex-valued functions. In [78], A. Aung et. al. proposed the properties of Complex Hadamard transform (CHT). Some variants have a sequency property that is similar to the DFT based on the unit circle. The following are variants of CHT.

Unified Complex Hadamard transform.

It is composed of integer-valued with unit Complex numbers [±1,±j] [149] and known as the Unified Complex Hadamard transform (UCHT). It was developed by S. Rahardja and B. J. Falkowski in 1999. UCHTs have been applied in spectral and logic design system tools [150]. According to the literature, the single unified formula generates 64 UCHTs matrices in total [Table 1, [149]]. The single Kronecker product or the direct matrix operator is used to create them. Exceptional half-spectrum property (HSP) is found in a small number of UCHTs [149][151][152]. HSP requires only half of the coefficients for computational analysis. The UCHT matrix equation is defined as below,

$$\mathbf{B}_1 = \mathbf{W}_1 \Diamond \begin{bmatrix} \psi_1 \\ \psi_2 \end{bmatrix} \Diamond [1 \quad \psi_3] \tag{3}$$

where W_1 is WHT matrix of order 2x2, and [■(ψ_1&ψ_2&ψ_3)] represents the complex values [149]. Unlike other variants of the CHT, it does not exhibit a specific ordering. The UCHT, however, possesses key properties such as orthogonality, unitarity, and symmetry. Table 1 presents the UCHT approaches for different applications.

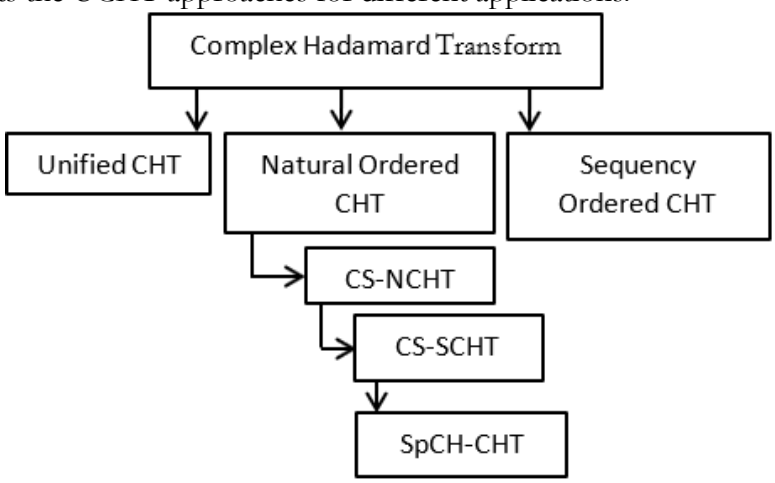

Figure 3. Family of Complex Hadamard Transform

Table 1. Unified Complex Hadamard Transform (UCHT) applications.

Ref.	Application	Approach	Findings
[153]	Boolean functions	A method for directly evaluating the UCHT spectra of AND, OR, and XOR for Boolean functions.	Decision diagrams are efficient representations of the spectra, and UCHT is discussed for image watermarking.
[149]	Implementation of UCHT matrix	A new type of discrete orthogonal transform was introduced.	The CHT's computational cost is cut in half due to the implementation of 64 matrices with half symmetry.
[154]	Asynchronous CDMA	The autocorrelation and cross-correlation are used to compare Gold, a small set of Kasami, and m-sequences in the presence of multiple access interference and AWGN.	In asynchronous direct sequence CDMA systems, BER performance comparisons of various spreading approaches with a half-spectrum property of the UCHT sequence have been shown.
[155]	S-SSMA	Based on the characteristic function approach, the average BER for quaternary asynchronous DS-SSMA systems with complex transmitters and receivers is calculated. The Gaussian approximation approach of multiple access interference is also used to get an approximate result.	Bit errors are less likely in synchronous DS-SSMA systems with UCHT sequences than in synchronous systems with non-orthogonal sequences. The results of simulations demonstrate that UCHT complex sequences can outperform the other two sequences.
[156]	CDMA	In DS-CDMA downlink systems, the orthogonal UCHT complex sequences are used. The system performance is measured using SINR at the RAKE receiver, and a generic multi-path fading channel model is employed.	The DS-CDMA downlink system's bit error ratio performance is improved when UCHT complex sequences are used, and it outperforms the system with WH sequences at high SINRs. The system's SINR is unaffected by phase offsets between various pathways.

Sequency Ordered-Complex Hadamard Transform.

In [78], the SCHT transformation matrix is classified into real and complex values. In the DFT, sequency is analogous to frequency. Fundamentally, the zero-crossings of the row vectors of both transforms are the same on the unit circle. As shown below, the SCHT transformation matrix is arranged on the complex version of the standard Rademacher function series (CRADM), which is confined on the unit circle with its parameters l and t on the normalized time base t∈[0,1) [79].

$$CRADM(l,t)=\begin{Vmatrix} 1, & [0,\frac{1}{4}) \\ j, & [\frac{1}{4},\frac{1}{2}) \\ -1, & [\frac{1}{2},\frac{3}{4}) \\ -j, & [\frac{3}{4},1) \end{Vmatrix} \quad (4)$$

where l are the discrete samples that represent the number of rows and t is mentioned for time base t [0,0.1,0.2,…..1). Steps for resultant SCHT transformation matrix have been presented as below.

- First, we need to find the Rth row matrix of dimension $n\times 2^n$.
- Determine the CRADM series for a particular value of l for each t sample.
- Fill the Rth row matrix for each row vector.
- In SCHT NxN order square matrix, the 1st row and column consist of DC value '1', and all other matrix elements depend on the Rth row matrix, which shows index values where binary digits with binary number '1'.

where the CRADM series and Rrth row matrix can be defined as,

$$CRADM(l,t)=CRADM(0,2^l t) \quad (5)$$

$$\mathbf{R}r_n(l,k)=CRADM(l,\frac{4k+1}{2^{n+2}}) \quad (6)$$

Where l=0,1…n-1 and k=0,1,…2^n-1, SCHT matrix can be expressed as,

$$\mathbf{H}_8^S(7,k)=[1,R_3(0),R_3(1),R_3(1)OR_3(0),R_3(2),.....,R_3(2)OR_3(1)OR_3(0)]' \quad (7)$$

Where O is the operator of element-by-element vector multiplications. The SCHT deals with complex valued functions, such as V_N $[v(0)…..v(N-1)]^T$.

$$V_N=\frac{1}{N}\bar{\mathbf{H}}_N^S v_N^T \quad (8)$$

The V_N is the transformed coefficient vector and $\bar{H}_N^S$ It is the conjugate matrix of SCHT. H_N^S. In the same way, the complex data vector can be retrieved by moving the SCHT matrix to the left-hand side. Table 2 shows the SCHT applications in different areas of signal processing and communication.

Table 2. Sequency Ordered Complex Hadamard Transform applications.

Ref.	Application	Approach	Findings
[78]	Properties and applications of SCHT	SCHT matrices are created using complex Rademacher matrices and reported in exponential form.	Estimation of the spectrum, analysis, and image watermarking are all implemented. The use of fast Fourier transforms (FFT) and the relationship between UCHT and SCHT are also discussed.
[157]	Asynchronous CDMA	For the A-CDMA system's performance, UCHT, WHT, Gold, a Small Set of Kasami, and m-sequences are used.	There are a variety of correlation properties offered. Over a multipath fading channel, SCHT yields better outcomes in terms of mean square cross-correlation and bit error rate.
[158]	Structure for pipelined hardware	An Algorithm is developed with decimation in sequence.	It's made for real-time applications that require complex additions and subtractions for $2(M-1)$ complex storage points.
[159]	Watermarking	The watermark coefficients were implemented using a phase modulation method.	Some attacking experiments were carried out to test the robustness of the proposed method, and it was found that it outperformed the others.
[160]	Fast sliding SCHT	It is described a forward and inverse fast SCHT sliding technique that compromises implementation and computational complexity.	It outperforms the block-based, sliding FFT, and DFT approaches. In the transform domain, adaptive filtering is also discussed.
[161]	Cognitive radio networks	For spectrum sensing, a Parzen window entropy approach with probability density estimation is proposed.	The proposed method used a signal-to-noise ratio of -54 dB and a probability detection of 0.9.
[162]	ECG-based Atrial fibrillation	Matrix factorization was done using the sparse approach.	SCHT has been employed for diagnostic applications.

Where H_N^N is a square and N^{th} order NCHT matrix that depends on $\mathbf{W}_{N/2}$ Walsh Walsh-Hadamard matrix. It can be produced by the right-hand side Kronecker product, where $N=2^n$ the lower half is multiplied by $\mathbf{S}$ a matrix. The matrix $\mathbf{S}$ will be given as $\mathbf{S}_{2^{n-1}}=\begin{bmatrix}\mathbf{I}_{2^{n-2}} & 0\\ 0 & j\mathbf{I}_{2^{n-2}}\end{bmatrix}$. NCHT deals with complex-valued functions such as

$$V_N=\frac{1}{N}\bar{\mathbf{H}}_N^N v_N^T \qquad (10)$$

where V_N is the transformed coefficient vector, and $\bar{\mathbf{H}}_N^N$ is the conjugate matrix of NCHT $\mathbf{H}_N^N$. The same complex data vector can be retrieved by moving the NCHT matrix to the left-hand side. Table 3 presents the applications of signal processing [80] of NCHT.

Complex Conjugate Sequency Ordered-Complex Hadamard Transform.

The frequency is known as the periodic repetition rate and rotation of the row vector of the DFT matrix on the normalised time $[0\le t\le 1]$ across the unit circle in the discrete Fourier transform DFT, and it has the conjugate symmetric property. A transform [81] that is the conjugate version of the SCHT and has a Sequency that is similar to the frequency of the DFT has been introduced. In terms of spectrum analysis, CS-SCHT outperforms SCHT since it only requires half of the spectral coefficients for signal analysis and synthesis.

The bit inverted order of the Conjugate Sequency – Natural Ordered Complex Hadamard Transform (CS-NCHT)is used to build the CS-SCHT. It is produced by using the WHT matrix. CS-NCHT is a square matrix $N=2^n$, it can be generated by two steps (but these steps work simultaneously for generating the CS-SCHT matrix).

The first step needs the upper half of the CS-NCHT matrix, while the second step requires the lower half of the CS-NCHT transform matrix [81] as given below,

$$\mathbf{H}_N^{CS-N}=\begin{bmatrix}\mathbf{W}_{N/2} & \mathbf{W}_{N/2}\\ \mathbf{W}''_{N/2}\mathbf{S}_{N/2} & -\mathbf{W}''_{N/2}\mathbf{S}_{N/2}\end{bmatrix} \qquad (11)$$

Step 1. Equation (11) is a similar matrix of the NCHT, for the upper half, the $\mathbf{W}_{N/2}$ is simply a WHT matrix. Step 2. The lower half of the CS-NCHT matrix $\mathbf{W}''_{N/2}$ is defined as,

$$\mathbf{W}''_{N/2}=\begin{bmatrix}\mathbf{W}''_{N/4} & \mathbf{W}''_{N/4}\\ \mathbf{W}''_{N/4}\mathbf{I}''_{N/4} & -\mathbf{W}''_{N/4}\mathbf{I}''_{N/4}\end{bmatrix} \qquad (12)$$

Where identity and S matrix can be formed as below, where the identity matrix is the nth element of the matrix and is multiplied by (-),

$$\mathbf{I}''_{2^{n-2}}=\begin{bmatrix}\mathbf{I}_{2^{n-3}} & 0\\ 0 & -\mathbf{I}_{2^{n-3}}\end{bmatrix} \qquad (13)$$

For the S matrix, where $N/2=2^{n-1}$

$$\mathbf{S}_{2^{n-1}}=\begin{bmatrix}\mathbf{I}_{2^{n-2}} & 0\\ 0 & j\mathbf{I}_{2^{n-2}}\end{bmatrix} \qquad (14)$$

For the CS-NCHT, insert equations (12-14) in equation (11). CS-SCHT transform matrix can be produced by the bit-reversed order of the CS-NCHT as,

$$\mathbf{H}_N^{CS-S}(m,k)=\mathbf{H}_N^{CS-N}(b(m),k) \qquad (15)$$

where m and k are the numbers of row and column vectors whose values depend on $0\le m,k\le N-1$ and $b(m)$ is the decimal value of the bit-reversed order. The CS-SCHT row vectors are in the increasing order of the unit circle on the complex plane, and the zeroth row and $N/2$ rows of the CS-SCHT correspond to the DC values and Nyquist rate in the DFT transform matrix.

Table 4. Conjugate Symmetry Sequency Ordered Complex Hadamard Transform applications.

Ref.	Application	Approach	Findings
[81]	CS-SCHT	The exponential properties and transformation matrix are derived. Shift-invariant dyadics are also investigated.	For spectrum estimation and image reduction, sparse matrix factorization was used.
[163]	Sliding CS-SCHT	A Fast CS-SCHT algorithm has been derived.	It is less efficient than WHT and performs better than the fast FFT technique. It's used for echo cancellation and single-channel equalization.
[164]	CS-DOT	The radix-2 approach is used to develop Fast DFT and Fast CS-SCHT, which are both special cases of the CS-DOT.	For real input signals, it has a conjugate-symmetric spectral structure. It costs half as much to store the data as it does to compute it.
[165]	Generalized CS-HT	The real-valued CHT was used to execute the simplified form of the closed-form factorization.	It yields some noteworthy results in terms of computing cost and memory needs for local orientations.
[166]	Signal processing	Sequency domain signal processing has been explored.	Frequency and sequency domain spectrum energy have been examined together with the image de-noising application.
[167]	Spatio-chromatic image processing	Spatio-chromatic CS-SCHT has been discussed by using CIE La*b* as a spatio-chromatic component.	In the frequency domain, colour paths have been examined and applied to colour images, with the resulting phasors seen for various inputs.
[168]	Signal processing	For multidimensional signal analysis, Quaternion CS-SCHT has been presented.	Color image applications have been explored using Quaternion CS-SCHT.
[169]	CS-SCHT for the gray code kernel	The current projection values were computed using the matrix tree approach.	Its computational cost is reduced with the comparison to the other Fast and Sling algorithms.
[170]	Watermarking	Spatio-chromatic watermarking is presented.	The watermarking results were compared to the spatio-chromatic DFT after the basis function was developed and presented.

Applications of CHT.

CHT has been employed in error coding approaches for the Hamming distance as error correction codes [171], and it was later provided as a generalized Complex WHT that was used in the error control mechanism [115]. UCHT was developed by B. J. Falkowski [149][152], and it has been used for the symmetry conditions of Boolean functions [172] and for the composite spectra of logic functions [153]. S. Rahardja introduced UCHT in the Code division multiplexing access techniques for asynchronous, Direct Sequence DS-CDMA and DS-spread spectrum multiplying access respectively [154][155][156], and it was shown that UCHT has a better BER performance than WHT.

To compare the usability and effectiveness of these trans- forms, many performance metrics have been created. The Dyadic Invariant Shift (DIS) fast SCHT technique cuts the computing cost of the SCHT transform greatly when compared to a direct computation [79]. A pipelined hardware structure has been built using SCHT that is applied with sequentially presented input/output data streams to facilitate high-speed real-time operations of the SCHT [158] by utilizing the concept of the DIS fast decomposition approach.

SCHT has been employed for asynchronous CDMA systems in 2007 [79][157], where it was compared to other m-sequences such as UCHT and WHT. SCHT was found to produce less mean square cross-correlation error at a fair degree of BER across multipath channel fading. SCHT has been used in signal and image processing/analysis [96][158][166][167][173][174][175] and linear algebra [176]. In comparison to DFT, sliding CS-SCHT has a lower computing cost for the real input signal, as shown in [[163] table (IV- V)], and it is used in a variety of applications [166][167][177].

Discrete orthogonal transform [164] is based on the CS-SCHT and DFT transforms. Complex values on the unit circle of the complex plane are used in both transforms. This is presented as a way to reduce both the computational and storage costs. The conjugate symmetric spectra for real input functions are provided by conjugate symmetric DOT. To create the CS-DOT, the CS-SCHT is used to set the twiddle factors. Therefore, the CS-DOT is a generalized and special case of both DFT and CS-SCHT. CS-DOT matrix as is given in [164], eq. 20].

In 2014, S. C. Pei [164] presented that the DOT provides more accurate results low computationally complex than CS-SCHT. The dominant lobe has more energy than CS-SCHT and is more closely linked to the DFT, which has applications in spectrum estimation. The arrangement of the hardware is based on the radix-2 butterfly as mentioned in [[164], Fig. 1]. In [165], a closed-form factorization based on complex and real-valued discrete transforms has been proposed. This sort of generic factorization was discovered to have a variety of benefits. Because it is conjugate symmetric, it has lower operational and computational costs, particularly in the case of real-valued CHT. Furthermore, memory is saved because this variation of CHT detects local image orientation. In [[165] Table II] shows the comparison is shown based on technical contents. It's used in applications like image coding and local orientation, where the real-valued CHT big block size outperforms the DFT. CHT is utilized in digital modulation, and it outperforms GSMK [178].

SCHT [161] was used for a cognitive radio network for the spectrum sensing in which the parezn window detection technique was compared with the conventional Shannon entropy method, and improvement was observed in SNR where the detection probability was 0.9 with a false probability of 0.1. In 2017 [177], phase domain video watermarking was proposed with low complexity, such as for high definition videos, in comparison with DFT. This method provides significant 37% savings of computations on hardware and provides better performance in PSNR, BER, and Mean Opinion Score (MOS). Table 5 presents the applications of CHT in different fields.

Fast CHT variants algorithms possess complex additions/subtractions and multiplication operations. Table 6 provides a comparison of computational cost for the different variants of CHT, and Table 7 presents the different properties of the CHT variants.

Table 5. Complex Hadamard Transform applications.

Ref.	Application	Approach	Findings
[152]	Boolean, multiple-valued logic functions.	Forward and inverse transformation kernels, as well as ways for recursively generating transform matrices utilizing Kronecker products of elementary matrices.	For arbitrary polarities, the link between transform matrices and spectra was presented. Decision diagrams and signal flow graphs are an efficient means of calculating spectra for logic functions.
[172]	Identification of symmetries in Boolean functions.	For CHTs based on complex Boolean spectra, the requirements for Boolean symmetries are established.	For the spectral technique, only the half-spectrum property is used to find symmetries in Boolean functions.
[115]	Generalized Reverse Jacket Transform (GRJT).	Presented a generalized transform entitled General Reverse Jacket Transform (GRJT) that unifies three classes of transforms, WHT, CWHT, and CRJT, by employing an appropriate mixed-radix representation of integers.	GRJT can be used to create error control codes. WHT, CWHT, and GRJT have all been briefly discussed.
[178]	Complex Hadamard matrix aided Generalized Space Shift Keying (HSSK)	Based on the Lee distance of signal vectors, HSSK delivers an optimal mapping between data bits and signal vectors. The average BER of the HSSK system's upper bound is also investigated.	Monte Carlo simulations are used to evaluate the performance of HSSK systems for Multiple Active-Spatial Modulation (MA-SM), Generalized Spatial Modulation (GSM), and Generalized Space Shift Keying (GSSK) systems. With the same transmission rates, HSSK systems outperform MA-SM, GSM, and GSSK systems in terms of BER. At the transmitter, complex Hadamard-based signal vectors outperform GSSK in terms of spectrum efficiency.
[171]	Error-correcting codes	Ternary Hadamard Codes and Exponent Generation	The matrix is known as a Classical Hadamard matrix when p=2 and the entries are all ±1. The Generalized Hadamard matrix is used when p>2.

[179]	Parameterizing matrices of Hadamard	To elevate affine parameterization, which leads to quantum applications, there are two techniques to generate CHTs with real values and conference matrices.	Two approaches are used to introduce CHTs with higher orders, i.e., 10, 12, and 14 for the affine parameterization relationship.
[176]	Construction of Hadamard matrices design for different parameterizations.	3 parameters have been used to develop the Hadamard matrices for 12 dimensions, which is the largest family.	Different matrix approaches have been performed using $\pm 1, \pm j$, Ø, and θ parameters.
[180]	New construction of equiangular tight frames using CH matrices	Different theorems have been proved using the signature matrix Q of an equiangular frame (n,k)	Matrices have been analyzed for linear algebra applications.
[174]	Classification of quaternary CH matrices	Butson-type Hadamard matrices BH (q, n) with q=4 and n=10, 12, and 14.	Matrices have been developed for the application of discrete mathematics.
[181][182][183][184]	nth -order circulant Hadamard matrices and convolutional neural networks (CNN)applications.	Construction of circulant Hadamard matrices for cyclic n-roots applications using distinct prime numbers.	Hadamard matrices have been analyzed using different distinct combinations of prime numbers. To use alternative 2D CNN layers for HT analysis.

Table 6. Computational cost of the variants of CHT.

Transform	Ref.	Value of N	Number of stages (n)	Complex Addition and Subtraction	Complex Multiplication	Reduction in computational cost
UCHT	[149]	$N = 2^n$	$log_2(N)$	-	-	-
Fast SCHT	[79]	$N = 2^n$	$log_2(N)$	$Nlog_2(N)$	$(N/4)log_2(N/2) = 2^{n-2}(n-1)$	$N(N-1)$
SCHT	[79]	$N = 2^n$	$log_2(N)$	$N(N-1)$ real	N^2 Real	-
F-CSSCHT	[81][182]	$N = 2^n$	$log_2(N)$	$Nlog_2(N)$	$(2^{n-1}-1)$	-
NCHT	[80]	$N = 2^n$	$log_2(N)$	$Nlog_2(N)$	$(N/4)log_2(N/2)$	$(N-1)/\ log_2(N)$

Table 7. Properties of CHT variants.

Transform	Ref.	Properties
UCHT	[149]	64 matrices, 32 half-spectrum property, 32 non-half-spectrum property with a value of $(\pm 1, \pm j)$
SCHT	[79]	Exponential Property, unitary, sequency, symmetry, and linearity
CSSCHT	[81]	Exponential Property, unitary, linearity, Parseval's theorem Conjugate symmetry, and Dyadic Shift Invariant Power Spectrum
NCHT	[80]	Exponential Property, unitary, linearity, Parseval's theorem, and shift-invariant power spectrum

Methodology.

The methodology defined in this survey paper serves as a framework for signal processing within the sequency domain, and is detailed as follows.

- A comprehensive compilation of the literature review sourced from various reputable platforms, encompassing transaction articles, scholarly books, correspondence, and conference proceedings.
- A systematic categorization of the transforms has been covered, including various real-valued WHT variants and classes of CHT. An evaluative comparison regarding computational cost, efficiency, normalization, and orthogonality within both the sequency and frequency domains.
- The implementation of these transforms has diverse categorizations in the field of signal processing. The challenges and limitations associated with WHT pertain to its functionality solely on the real axis, while CHT operates on both real and imaginary components, analogous to DFT, although restricted to the boundaries of the quadrants.
- Prospective advancements for both real and complex HT's suggest their application to fractional transforms such as DFT, with potential integration into CNN applications. The methodology is presented in Figure 4.

Figure 4. Flow of study diagram

The process of the methodology is discussed below.

To accomplish a thorough literature review related to the WHT and CHT, the process is initiated by aggregating data from reputable academic repositories such as IEEE Xplore, SpringerLink, ScienceDirect, and the ACM Digital Library. Following the compilation of appropriate data, the transforms were systematically categorized into two primary classifications. real-valued (WHT) and complex-valued (CHT). The WHT is distinguished by its binary characteristics, consisting of matrix elements of +1 and -1, thereby rendering it particularly suitable for hardware implementations. Conversely, the CHT encompasses complex roots of unity and is conventionally unitary, which enables the preservation of signal energy within the complex domain. CHT matrices are frequently utilized in more sophisticated

applications, such as quantum circuits and secure communication systems. This classification was executed based on their mathematical attributes, computational frameworks, and respective areas of application.

A rigorous technical analysis was subsequently executed to assess and contrast the computational cost and operational efficiency of these transformations. Evaluative metrics such as algorithmic complexity, hardware compatibility, numerical stability, and energy conservation were systematically examined. Both the WHT and the CHT typically exhibit a complexity of $O(N)log(N)$. Experimental simulations conducted utilizing MATLAB assessed the performance of the transforms using gray images, encompassing one-dimensional signals and two-dimensional images. This comparative analysis elucidated that, although the DCT and DFT are more commonly employed in image and audio compression standards (e.g., JPEG and MP3), the WHT confers advantages in terms of computational speed and binary implementation efficiency. The CHT, despite its increased complexity, excels in quantum processing and intricate signal applications attributable to its unitary nature and robustness. Tabulated comparisons were constructed to evaluate compression efficiency, signal fidelity (measured via Peak Signal-to-Noise Ratio, PSNR), and utility specific to various applications.

Eventually, the applications of the WHT and CHT were investigated to explain their impact across multiple domains. The WHT has demonstrated efficacy in fault detection, spectral analysis, and compression, particularly within low-power embedded systems. Conversely, the CHT has identified promising applications in the realm of quantum computing, phase-based encryption methodologies, and secure signal processing techniques. Existing literature suggests that WHT-based methodologies achieve substantial noise reduction and compression with moderate losses in PSNR, while CHT-based approaches excel in complex scenarios necessitating enhanced security and precision. The review culminated with a discourse on the trade-offs between complexity and performance, affirming that the selection of the appropriate transform should be customized to the specific application domain.

Results.

In the domains of signal processing and spectrum estimation, the CHT and its various extensions served as powerful tools for frequency-domain analysis. Figure 5 presents the magnitude response characteristics of several CHT variants (as shown in subfigures 5a–5f), using normalized sequences based on N=8-point transform matrices. Each subfigure corresponded to the magnitude response across normalized frequency for individual row vectors of the respective 8×8 transformation matrices. The analysis revealed distinct frequency behaviors across the transform variants. Notably, the Diagonal Orthogonal Transform-based CHT (DOT-CHT) demonstrates a frequency response pattern that closely mirrors that of the Discrete Fourier Transform (DFT), as supported by comparisons drawn from literature. This strong resemblance indicated that DOT-CHT retained desirable spectral properties akin to the DFT, making it a viable alternative in applications where computational efficiency and structural simplicity are prioritized.

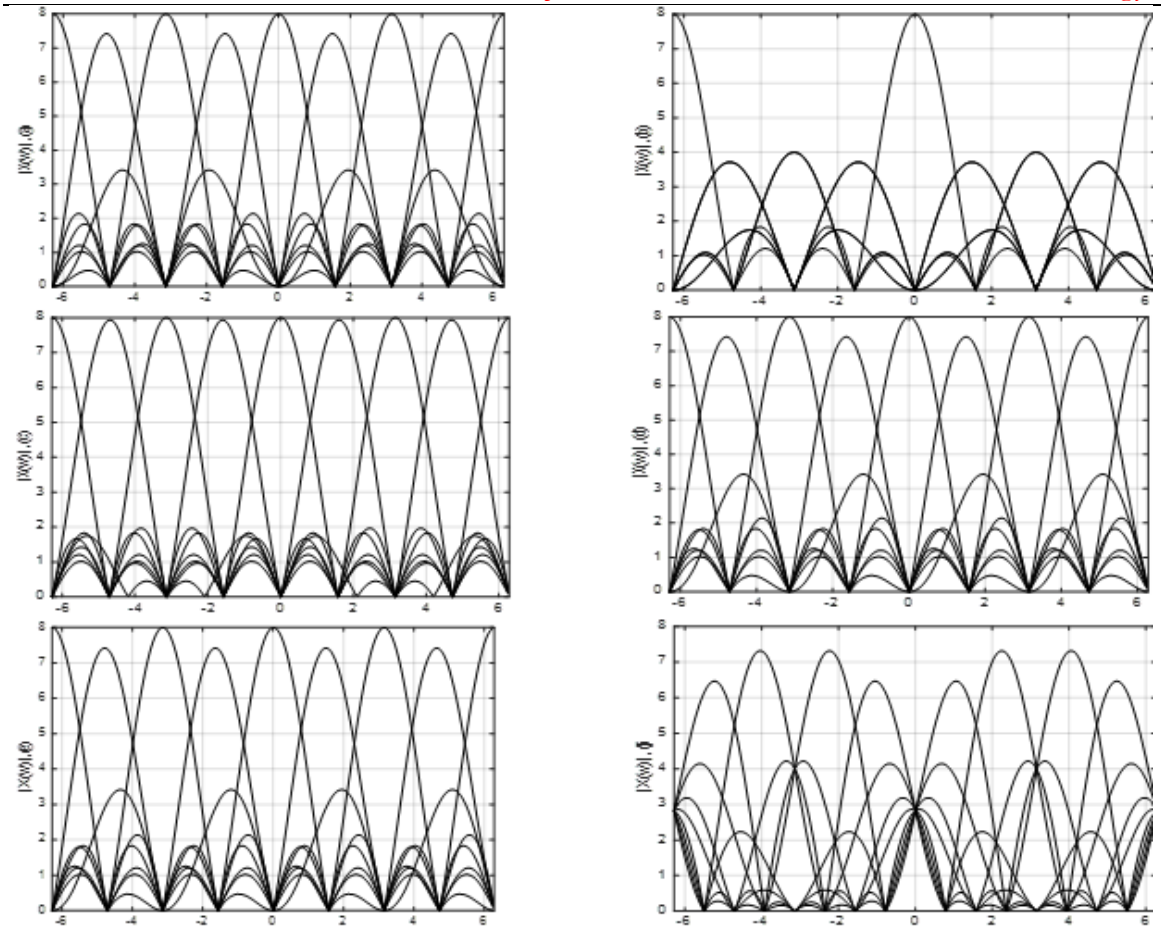

Figure 5. Normalized sequences are presented for the magnitude responses of CHT matrices for N=8. (a) CSSCHT, (b) rCSSCHT, (c) DOTCHT, (d) SCHT, (e) NCHT, (f) UCHT (HSP).

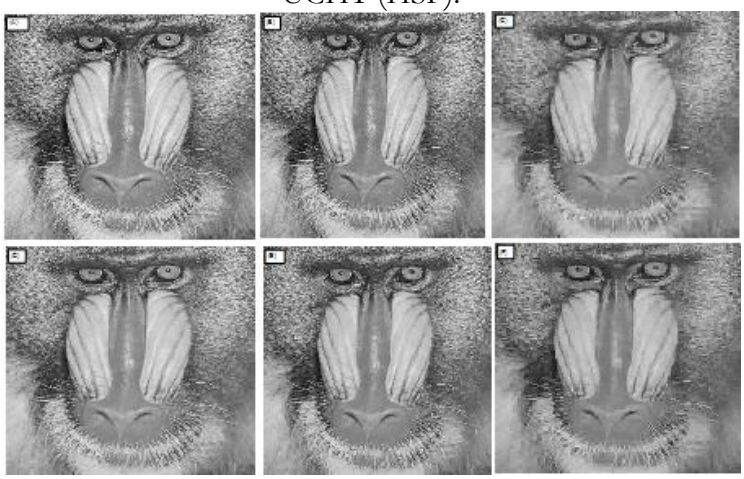

Figure 6. Image compression using variants of CHTs. a) Original image. b) UCHT. c) NCHT. d) SCHT. e) CSSCHT. f) DOT-CHT.

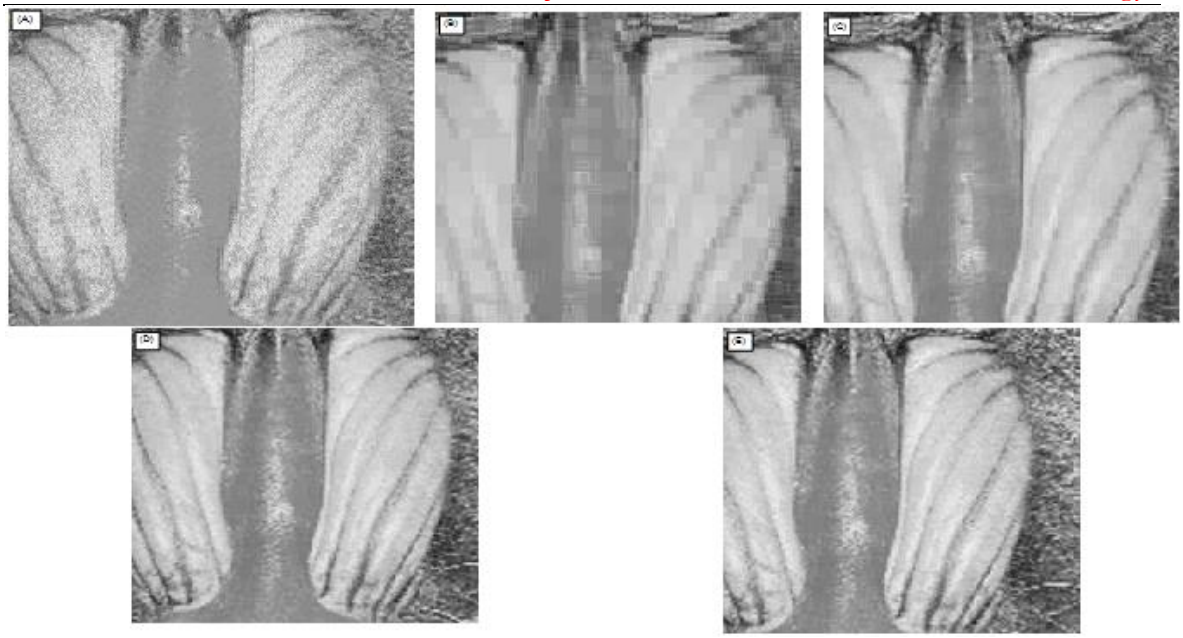

Figure 7. Zoomed compressed images of the Figure. 6. a) UCHT. b) NCHT. c) SCHT. d) CSSCHT. e) DOT-CHT

Moreover, the performance of the various CHT variants exhibited noticeable inconsistencies. Among these, the UCHT showed a distinct behavior in its frequency response, with all frequency components starting from different points compared to the other CHT variants. This irregularity resulted in more prominent and undesired sidebands in the magnitude spectra, thereby affecting the spectral quality of the transform. Despite these limitations, complex Hadamard transforms had significant applications in signal processing and image compression. Their importance was due to their reliance on arithmetic operations and the sequency-based ordering present in most CHTs, except in the case of UCHT, which lacked this property. These characteristics made them effective tools for data reduction and compression. This was illustrated in the figures. Figure 6a presented the original 256×256 grayscale image of a baboon, while Figures 6b to 6f, aligned horizontally, showed the corresponding compressed outputs using different CHT variants. For a closer inspection of the compression quality, zoomed-in versions of these images were displayed in Figure 7.

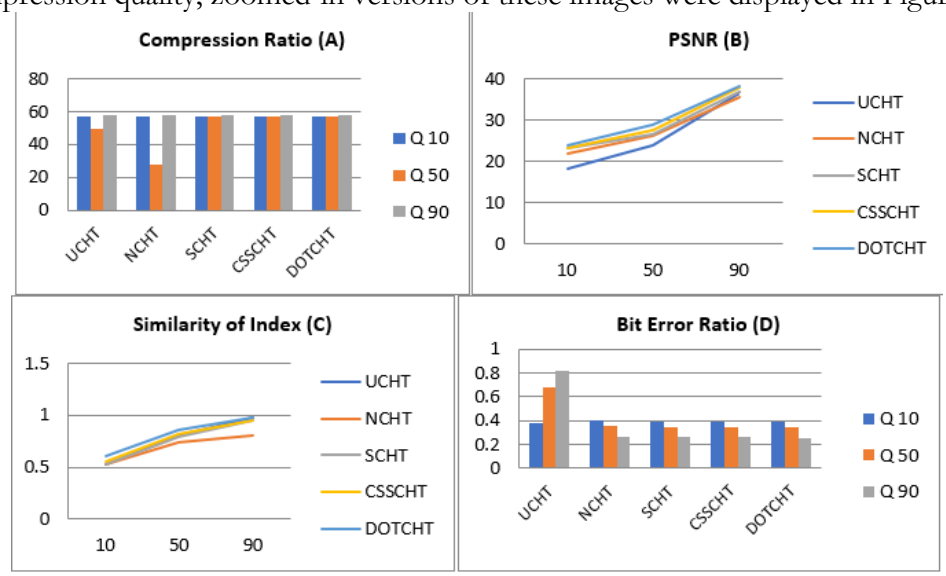

Figure 8. (a) Comparison vs quantization matrix. (b) PSNR vs quantization matrix. (c) Similarity of index vs quantization matrix. (d) Bit error ratio vs compression ratio.

The visual and quantitative evaluation of compressed images using various Complex Hadamard Transform (CHT) variants revealed notable differences in image quality and performance metrics. Figures 7a–7c illustrate the reconstructed images after compression, where visible blocky artifacts are observed across most transforms. However, the CS-SCHT and DOT-CHT variants produce superior results, it is showing significantly reduced block-based distortions and higher visual fidelity. In contrast, the images reconstructed using UCHT and NCHT exhibit pronounced deformation, with UCHT showing the most degradation among all variants.

To further quantify performance, Figure 8 presents a comparative analysis of image compression metrics, compression ratio, Peak Signal-to-Noise Ratio (PSNR), Structural Similarity Index (SSIM), and Bit Error Ratio (BER) under varying quantization matrices (Q = 10, 50, and 90). The results demonstrated that UCHT is highly sensitive to compression, resulting in lower PSNR and SSIM values and higher BER. NCHT also experienced degradation due to compression, though less severe than UCHT. In contrast, SCHT, CS-SCHT, and DOT-CHT exhibited strong resilience to quantization, maintaining stable PSNR, SSIM, and BER values across all Q levels, as shown in Figures 8a through 8d.

Overall, the study highlights that certain CHT variants, particularly CS-SCHT and DOT-CHT, offer enhanced robustness and image quality under compression, making them suitable for a wide range of applications in scientific and engineering domains where efficient and reliable image representation is critical.

Discussion.

The analysis of CHT's reveals key insights into their utility and limitations in signal and image processing, particularly when compared to established methods such as the DFT and DCT. The statement highlights a significant observation, such as inconsistency in the spectral response of CHT variants, especially UCHT. Unlike other CHT variants that exhibit consistent sequency ordering (a measure of frequency content in basis vectors), the UCHT shows deviation at the initial frequency indices, leading to non-uniform spectral energy distribution. This results in undesirable sidebands, a phenomenon where energy leaks into unintended frequency bins, reducing the efficiency and quality of signal representation. Such effects are detrimental in applications like compression, where preserving important spectral features is crucial. By contrast, DFT maintains a fixed and interpretable frequency ordering, but its complex-valued basis can make computations relatively costly (multiplications with real and imaginary components). It does not optimize for energy compaction, which limits its use in image compression unless combined with other methods. DCT, on the other hand, is renowned for its energy compaction properties, especially in low-frequency components, which makes it ideal for image compression (as seen in JPEG). It is a real-valued transform, meaning it avoids complex arithmetic, unlike both DFT and CHT. The DCT's basis functions are cosine-only, contributing to smooth, block-based approximations that are visually less disruptive than high-frequency variations caused by poor transform design. In this context, CHT variants (excluding UCHT) provide a valuable middle ground as they preserve sequency ordering like DCT and are efficient due to their reliance on only arithmetic operations (e.g., additions, subtractions, and multiplications by ± 1 or $\pm j$). This makes them suitable for hardware implementations and low-latency applications. Moreover, their complex domain properties offer unique flexibility in encoding phase and amplitude information, beneficial in areas like watermarking, holography, and multi-dimensional filtering. The reference to Figure 6, a set of compressed images, further emphasizes practical outcomes. Visual inspection of images from different CHT variants reveals that compression artifacts, such as blockiness and blurring, vary significantly. UCHT introduces more distortion, while DOT-CHT and CS-SCHT preserve details more effectively, with sideband minimization and better visual fidelity.

The analysis provided in Figure 8 focuses on key image compression metrics, Compression Ratio, SSIM, and BER under varying levels of quantization (Q = 10, 50, 90). These metrics collectively reflect the effectiveness of a transformation technique in preserving image quality under compression. The results provide significant insights into how different CHT variants behave under compression stress and how they compare to traditional techniques such as the DFT and DCT.

Performance of UCHT and NCHT. The UCHT stands out as the least robust of the CHT variants, showing clear performance degradation with increasing quantization. Its lower PSNR and SSIM values indicate visible distortion and poorer structural fidelity in reconstructed images. The high BER further highlights a loss of pixel-level accuracy. This sensitivity is likely due to the lack of proper sequence ordering and its inconsistent spectral behavior, which can lead to inefficient quantization and reconstruction. NCHT performs better than UCHT but still shows susceptibility to compression artifacts. This partial instability implies that while NCHT has potential for signal representation, its robustness under heavy quantization is limited.

Robustness of SCHT, CS-SCHT, and DOT-CHT. On the other hand, SCHT, CS-SCHT, and DOT-CHT consistently maintain high PSNR and SSIM values and low BER, even as the quantization matrix becomes more aggressive (from Q = 90 to Q = 10). This demonstrates their quantization resilience, making them more suitable for applications requiring high compression efficiency without sacrificing image quality. The reason lies in their optimized sequence order and arithmetic-only design, which allows for better energy compaction and minimized signal distortion during quantization and reconstruction.

Conclusion.

The family of Complex Hadamard transforms and its applications are presented in this study. The number of variants has been implemented and thoroughly debated. Each version has its characteristics and significance in various fields of signal processing and communication. When used to signal analysis/synthesis, the results show that SCHT, CSSCHT, and DOT-CHT perform similarly to DFT. Image compression is better with DOT-CHT and CSSCHT. In communication applications, UCHT and SCHT are also used and show better performance. NCHT is yet to be thoroughly investigated. In image and spectral analysis, SCHT and CSSCHT are commonly used.

CSSCHT has a sequence attribute like DFT's frequency, and it can be used in a variety of applications due to its lower computational cost. Different CHTs' normalized magnitude spectrum was observed and discussed. The CSSCHT and DOT-CHT exhibit fewer blocky artefacts due to their sequency feature, which has been found in image compression for CHT variations. If referred to base on the quality vs. computational cost tradeoff. CHTs can be used in a wide range of scientific areas and for a wide range of applications.

References.

[1] Melisew Tefera Belachew, "Efficient algorithm for sparse symmetric nonnegative matrix factorization," Pattern Recognit. Lett., vol. 125, pp. 735–741, 2019, [Online]. Available. https.//www.sciencedirect.com/science/article/abs/pii/S0167865519302132?via%3Dihub

[2] D. S. P. and M. H. L. Y. Guo, Y. Mao, "Fast DFT matrices transform based on generalized prime factor algorithm," J. Commun. Networks, vol. 13, no. 5, pp. 449–455, 2011, [Online]. Available. https.//ieeexplore.ieee.org/document/6112301

[3] Zhenjun, T., "Robust image hashing via colour vector angles and discrete wavelet transform," Image Process., vol. 8, no. 3, pp. 142–149, 2014, [Online]. Available. https.//ietresearch.onlinelibrary.wiley.com/doi/epdf/10.1049/iet-ipr.2013.0332

[4] Z. P. Lingma Sun, Zhuoran Wang, Hong Pu, Guohui Yuan, Lu Guo, Tian Pu, "Spectral analysis for pulmonary nodule detection using the optimal fractional S-Transform," Comput. Biol. Med., vol. 119, p. 103675, 2020, [Online]. Available.

https://www.sciencedirect.com/science/article/abs/pii/S0010482520300676?via%3Dihub
[5] W. Li, J. Li, X. Liu, and L. Dong, "Two fast vector-wise update algorithms for orthogonal nonnegative matrix factorization with sparsity constraint," J. Comput. Appl. Math., vol. 375, p. 112785, 2020, doi. https://doi.org/10.1016/j.cam.2020.112785.
[6] V. F. Lorenzo Valdettaro, Michel Rieutord, Thierry Braconnier, "Convergence and round-off errors in a two-dimensional eigenvalue problem using spectral methods and Arnoldi–Chebyshev algorithm," J. Comput. Appl. Math., vol. 205, no. 1, pp. 382–393, 2007, doi. https://doi.org/10.1016/j.cam.2006.05.009.
[7] S. B. Cooper and J. Van Leeuwen, "Rounding-off Errors in Matrix Processes," Alan Turing His Work Impact, pp. 377–402, 2013, [Online]. Available. https://www.sciencedirect.com/science/article/abs/pii/B9780123869807500150?via%3Dihub
[8] E. A. N. M.H. Annaby, H.A. Ayad, M.A. Rushdi, "Difference operators and generalized discrete fractional transforms in signal and image processing," Signal Processing, vol. 151, pp. 1–18, 2018, doi. https://doi.org/10.1016/j.sigpro.2018.04.023.
[9] C. T. Alejandro Gómez-Echavarría, Juan P. Ugarte, "The fractional Fourier transform as a biomedical signal and image processing tool. A review," Biocybern. Biomed. Eng., vol. 40, no. 3, pp. 1081–1093, 2020, doi. https://doi.org/10.1016/j.bbe.2020.05.004.
[10] Lan, R., "Multiple-Action Transform of Quaternion for Color Images," IEEE Access, vol. 7, pp. 124283–124294, 2019, [Online]. Available. https://ieeexplore.ieee.org/document/8819965/
[11] A. I. Zahraa Ch. Oleiwi, Dhiah Al-Shammary, Muntasir Al-Asfoor, "Light network high performance discrete cosine transform for digital images," Vis. Informatics, vol. 5, no. 2, pp. 41–50, 2021, doi. https://doi.org/10.1016/j.visinf.2021.06.001.
[12] N. Roma and L. Sousa, "A tutorial overview on the properties of the discrete cosine transform for encoded image and video processing," Signal Processing, vol. 91, no. 11, pp. 2443–2464, 2011, doi. https://doi.org/10.1016/j.sigpro.2011.04.015.
[13] T. C. Hsung, D. P. K. Lun, and W. C. Siu, "A deblocking technique for block-transform compressed image using wavelet transform modulus maxima," IEEE Trans. Image Process., vol. 7, no. 10, pp. 1488–1496, 1998, doi. 10.1109/83.718489.
[14] X. Wang, "Moving window-based double haar wavelet transform for image processing," IEEE Trans. Image Process., vol. 15, no. 9, pp. 2771–2779, Sep. 2006, doi. 10.1109/TIP.2006.877316.
[15] G. Xu, K. Liu, C. Guo, and Q. Wang, "Natural-ordered complex hadamard transform based shape description and retrieval," Proc. - 2014 6th Int. Conf. Intell. Human-Machine Syst. Cybern. IHMSC 2014, vol. 2, pp. 55–58, Sep. 2014, doi. 10.1109/IHMSC.2014.116.
[16] Z. L. and X. X. X. Zeng, "A Fast Fusion Method for Visible and Infrared Images Using Fourier Transform and Difference Minimization," IEEE Access, vol. 8, pp. 213682–213694, 2020, doi. 10.1109/ACCESS.2020.3041759.
[17] P. Zheng and J. Huang, "Efficient Encrypted Images Filtering and Transform Coding with Walsh-Hadamard Transform and Parallelization," IEEE Trans. Image Process., vol. 27, no. 5, pp. 2541–2556, May 2018, doi. 10.1109/TIP.2018.2802199.
[18] Andrzej Dziech, "New Orthogonal Transforms for Signal and Image Processing," Appl. Sci., vol. 11, no. 16, p. 7433, 2021, doi. https://doi.org/10.3390/app11167433.
[19] P. G. Freitas, W. Y. L. Akamine, and M. C. Q. Farias, "No-Reference Image Quality Assessment Using Orthogonal Color Planes Patterns," IEEE Trans. Multimed., vol. 20, no. 12, pp. 3353–3360, 2018, doi. 10.1109/TMM.2018.2839529.
[20] S. Rousseau and D. Helbert, "Compressive Color Pattern Detection Using Partial Orthogonal Circulant Sensing Matrix," IEEE Trans. Image Process., vol. 29, pp. 670–678, 2020, doi. 10.1109/TIP.2019.2927334.
[21] B. K. L. Isio Sota-Uba, Matthew Bamidele, James Moulton, Karl Booksh, "Authentication of edible oils using Fourier transform infrared spectroscopy and pattern recognition methods," Chemom. Intell. Lab. Syst., vol. 210, p. 104251, 2021, doi.

https://doi.org/10.1016/j.chemolab.2021.104251.
[22] A. S. Turker Tuncer, Sengul Dogan, "Surface EMG signal classification using ternary pattern and discrete wavelet transform based feature extraction for hand movement recognition," Biomed. Signal Process. Control, vol. 58, p. 101872, 2020, doi. https://doi.org/10.1016/j.bspc.2020.101872.
[23] X. You and Y. Y. Tang, "Wavelet-based approach to character skeleton," IEEE Trans. Image Process., vol. 16, no. 5, pp. 1220–1231, May 2007, doi. 10.1109/TIP.2007.891800.
[24] T. Wakahara and K. Odaka, "Adaptive normalization of handwritten characters using global/local affine transformation," IEEE Trans. Pattern Anal. Mach. Intell., vol. 20, no. 12, pp. 1332–1341, 1998, doi. 10.1109/34.735806.
[25] B. Hadjadji, Y. Chibani, and H. Nemmour, "An efficient open system for offline handwritten signature identification based on curvelet transform and one-class principal component analysis," Neurocomputing, vol. 265, pp. 66–77, 2017, [Online]. Available. https://www.sciencedirect.com/science/article/abs/pii/S0925231217310159?via%3Dihub
[26] B. Y. H. Shih Yin Ooi, Andrew Beng Jin Teoh, Ying Han Pang, "Image-based handwritten signature verification using hybrid methods of discrete Radon transform, principal component analysis and probabilistic neural network," Appl. Soft Comput., vol. 40, pp. 274–282, 2016, [Online]. Available. https://www.sciencedirect.com/science/article/abs/pii/S1568494615007577?via%3Dihub
[27] S. Rashidi, A. Fallah, and F. Towhidkhah, "Feature extraction based DCT on dynamic signature verification," Sci. Iran., vol. 19, no. 6, pp. 1810–1819, 2012, doi. https://doi.org/10.1016/j.scient.2012.05.007.
[28] C.-H. Y. Assaidah Adnan, Yang Liu, Chi-Wai Chow, "Analysis of Non-Hermitian symmetry (NHS) IFFT/FFT size efficient OFDM for multiple-client non-orthogonal multiple access (NOMA) visible light communication (VLC) system," Opt. Commun., vol. 472, p. 125991, 2020, [Online]. Available. http.//sciencedirect.com/science/article/abs/pii/S0030401820304211?via%3Dihub
[29] M. Chen, H. Lu, D. Chen, J. Jin, and J. Wang, "An efficient MIMO–OFDM VLC system of combining space time block coding with orthogonal circulant matrix transform precoding," Opt. Commun., vol. 473, p. 125993, 2020, [Online]. Available. https://www.sciencedirect.com/science/article/abs/pii/S0030401820304223?via%3Dihub
[30] F. Cruz-Roldan, W. A. Martins, P. S. R. Diniz, and M. Moonen, "Achievable Data Rate of DCT-Based Multicarrier Modulation Systems," IEEE Trans. Wirel. Commun., vol. 18, no. 3, pp. 1739–1749, Mar. 2019, doi. 10.1109/TWC.2019.2896073.
[31] F. E. A. E.-S. K. Ramadan, Moawad I. Dessouky, "Joint equalization and CFO compensation for performance enhancement of MIMO-OFDM communication systems using different transforms with banded-matrix approximation," AEU - Int. J. Electron. Commun., vol. 119, p. 153157, 2020, [Online]. Available. https://www.sciencedirect.com/science/article/abs/pii/S1434841119318795?via%3Dihub
[32] F. E. A. E.-S. K. Ramadan, Moawad I. Dessouky, "Modified OFDM configurations with equalization and CFO compensation for performance enhancement of OFDM communication systems using symmetry of the Fourier transform," AEU - Int. J. Electron. Commun., vol. 126, p. 153247, 2020, [Online]. Available. https://www.sciencedirect.com/science/article/abs/pii/S1434841119323453?via%3Dihub
[33] R. H. Damoon Shahbaztabar, Shahpour Alirezaee, Majid Ahmadi, "A MC-CDMA system based on orthogonal filter banks of wavelet transforms and partial combining," AEU - Int. J. Electron. Commun., vol. 94, pp. 128–138, 2018, [Online]. Available. https://www.sciencedirect.com/science/article/abs/pii/S1434841117327103?via%3Dihub
[34] Z. W. and J. Z. Y. Yu, W. Wang, X. Ouyang, "Sparse Orthogonal Circulant Transform Multiplexing for Coherent Optical Fiber Communication," IEEE Photonics J., vol. 10, no. 1, pp. 1–14, 2018, doi. 10.1109/JPHOT.2018.2796846.
[35] S. Aathilakshmi, R. Vimala, and K. R. A. Britto, "An elegance of novel digital filter using

majority logic on pipelined architecture for SNR improvement in signal processing," J. Ambient Intell. Humaniz. Comput., pp. 1–9, Apr. 2021, doi. 10.1007/S12652-021-03197-7/METRICS.
[36] K. Ichige, M. Iwaki, and R. Ishii, "Accurate estimation of minimum filter length for optimum FIR digital filters," IEEE Trans. Circuits Syst. II Analog Digit. Signal Process., vol. 47, no. 10, pp. 1008–1016, 2000, doi. 10.1109/82.877143.
[37] P. J. Ahamed and M. A. Haseeb, "Implementation of digital IIR filter design based on field programmable gate array," Mater. Today Procedding, vol. 45, no. 2, pp. 2573–2577, 2021, doi. https://doi.org/10.1016/j.matpr.2020.11.273.
[38] P. Löwenborg, H. Johansson, and L. Wanhammar, "Two-channel digital and hybrid analog/digital multirate filter banks with very low-complexity analysis or synthesis filters," IEEE Trans. Circuits Syst. II Analog Digit. Signal Process., vol. 50, no. 7, pp. 355–367, Jul. 2003, doi. 10.1109/TCSII.2003.813589.
[39] M. K. Suman Yadav, Richa Yadav, Ashwni Kumar, "A novel approach for optimal design of digital FIR filter using grasshopper optimization algorithm," ISA Trans., vol. 108, pp. 196–206, 2021, [Online]. Available. https://www.sciencedirect.com/science/article/abs/pii/S0019057820303645?via%3Dihub
[40] N. N. Pavel Lyakhov, Maria Valueva, Georgii Valuev, "A Method of Increasing Digital Filter Performance Based on Truncated Multiply-Accumulate Units," Appl. Sci., vol. 10, no. 24, p. 9052, 2020, doi. https://doi.org/10.3390/app10249052.
[41] J. P. Jean-Jacques Vandenbussche, Peter Lee, "Round-Off Noise of Multiplicative FIR Filters Implemented on an FPGA Platform," Appl. Sci., vol. 4, no. 2, pp. 99–127, 2014, doi. https://doi.org/10.3390/app4020099.
[42] Z. Khalid, S. Durrani, P. Sadeghi, and R. A. Kennedy, "Spatio-spectral analysis on the sphere using spatially localized spherical harmonics transform," IEEE Trans. Signal Process., vol. 60, no. 3, pp. 1487–1492, Mar. 2012, doi. 10.1109/TSP.2011.2177265.
[43] J.-M. K. Sacha Lapins, Diana C. Roman, Jonathan Rougier, Silvio De Angelis, Katharine V. Cashman, "An examination of the continuous wavelet transform for volcano-seismic spectral analysis," J. Volcanol. Geotherm. Res., vol. 389, p. 106728, 2020, [Online]. Available. https://www.sciencedirect.com/science/article/abs/pii/S0377027319303051?via%3Dihub
[44] C. H. Paik, G. L. Cote, J. S. DaPonte, and M. D. Fox, "Fast Hartley Transforms for Spectral Analysis of Ultrasound Doppler Signals," IEEE Trans. Biomed. Eng., vol. 35, no. 10, pp. 885–888, 1988, doi. 10.1109/10.7298.
[45] Q. Q. Jun Xu, Bingliang Hu, Dazheng Feng, Xiaohui Fan, "Analysis and study of the interlaced encoding pixels in Hadamard transform spectral imager based on DMD," Opt. Lasers Eng., vol. 50, no. 3, pp. 458–464, 2012, doi. https://doi.org/10.1016/j.optlaseng.2011.10.007.
[46] H. Hosseini-Nejad, A. Jannesari, and A. M. Sodagar, "Data compression in brain-machine/computer interfaces based on the walsh-hadamard transform," IEEE Trans. Biomed. Circuits Syst., vol. 8, no. 1, pp. 129–137, 2014, doi. 10.1109/TBCAS.2013.2258669.
[47] C. K. Jha and M. H. Kolekar, "Electrocardiogram data compression using DCT based discrete orthogonal Stockwell transform," Biomed. Signal Process. Control, vol. 46, pp. 174–181, 2018, doi. https://www.sciencedirect.com/science/article/abs/pii/S1746809418301617?via%3Dihub.
[48] M. Morháč and V. Matoušek, "Fast adaptive Fourier-based transform and its use in multidimensional data compression," Signal Processing, vol. 68, no. 2, pp. 141–153, 1998, [Online]. Available. https://www.sciencedirect.com/science/article/abs/pii/S0165168498000693?via%3Dihub
[49] P. W. Shaofei Dai, Wenbo Liu, Zhengyi Wang, Kaiyu Li, Pengfei Zhu, "An Efficient Lossless Compression Method for Periodic Signals Based on Adaptive Dictionary Predictive Coding," Appl. Sci., vol. 10, no. 14, p. 4918, 2020, doi. https://doi.org/10.3390/app10144918.
[50] I. Pitas and A. Karasaridis, "Multichannel transforms for signal/image processing," IEEE Trans. Image Process., vol. 5, no. 10, pp. 1402–1413, 1996, doi. 10.1109/83.536889.
[51] J. F. Barmak Honarvar Shakibaei Asli, "New discrete orthogonal moments for signal

analysis," Signal Processing, vol. 141, pp. 57–73, 2017, doi. https://doi.org/10.1016/j.sigpro.2017.05.023.
[52] Rodrigo Capobianco Guido, "Nearly symmetric orthogonal wavelets for time-frequency-shape joint analysis. Introducing the discrete shapelet transform's third generation (DST-III) for nonlinear signal analysis," Commun. Nonlinear Sci. Numer. Simul., vol. 97, p. 105685, 2021, doi. https://doi.org/10.1016/j.cnsns.2020.105685.
[53] David Brandwood, "Fourier Transforms in Radar and Signal Processing, Second Edition," ARTECH House, p. 262, 2011, [Online]. Available. https://us.artechhouse.com/Fourier-Transforms-in-Radar-and-Signal-Processing-Second-Edition-P1497.aspx
[54] H. S. Stone, "Convolution theorems for linear transforms," IEEE Trans. Signal Process., vol. 46, no. 10, pp. 2819–2821, 1998, doi. 10.1109/78.720385.
[55] S. C. Pei, J. H. Chang, and J. J. Ding, "Commutative reduced biquaternions and their Fourier transform for signal and image processing applications," IEEE Trans. Signal Process., vol. 52, no. 7, pp. 2012–2030, Jul. 2004, doi. 10.1109/TSP.2004.828901.
[56] S. C. Pei, J. J. Ding, and J. H. Chang, "Efficient implementation of quaternion Fourier transform, convolution, and correlation by 2-D complex FFT," IEEE Trans. Signal Process., vol. 49, no. 11, pp. 2783–2797, Nov. 2001, doi. 10.1109/78.960426.
[57] Z. Yan, P. Chao, J. Ma, D. Cheng, and C. Liu, "Discrete convolution wavelet transform of signal and its application on BEV accident data analysis," Mech. Syst. Signal Process., vol. 159, p. 107823, 2021, doi. https://doi.org/10.1016/j.ymssp.2021.107823.
[58] A. Spriet, M. Moonen, and J. Wouters, "Robustness analysis of Multichannel Wiener filtering and generalized sidelobe cancellation for multimicrophone noise reduction in hearing aid applications," IEEE Trans. Speech Audio Process., vol. 13, no. 4, pp. 487–503, Jul. 2005, doi. 10.1109/TSA.2005.845821.
[59] W. K. Pratt, "Generalized Wiener Filtering Computation Techniques," IEEE Trans. Comput., vol. C–21, no. 7, pp. 636–641, 1972, doi. 10.1109/T-C.1972.223567.
[60] C. M. Wennian Yu, Yimin Shao, Jin Xu, "An adaptive and generalized Wiener process model with a recursive filtering algorithm for remaining useful life estimation," Reliab. Eng. Syst. Saf., vol. 217, p. 108099, 2022, doi. https://doi.org/10.1016/j.ress.2021.108099.
[61] R. T. Hilger, R. E. Santini, and S. A. McLuckey, "Square wave modulation of a mirror lens for ion isolation in a Fourier transform electrostatic linear ion trap mass spectrometer," Int. J. Mass Spectrom., vol. 362, pp. 1–8, 2014, doi. https://doi.org/10.1016/j.ijms.2014.02.003.
[62] Stephen A. Dyer, "Hadamard transform spectrometry," Chemom. Intell. Lab. Syst., vol. 12, no. 2, pp. 101–115, 1991, doi. https://doi.org/10.1016/0169-7439(91)80119-B.
[63] C. N. Li, G. R. Hu, and M. J. Liu, "Narrow-band interference excision in spread-spectrum systems using self-orthogonalizing transform-domain adaptive filters," IEEE J. Sel. Areas Commun., vol. 18, no. 3, pp. 403–406, Mar. 2000, doi. 10.1109/49.840199.
[64] Z. Lu, J. Sun, and K. Butts, "Multiscale asymmetric orthogonal wavelet kernel for linear programming support vector learning and nonlinear dynamic systems identification," IEEE Trans. Cybern., vol. 44, no. 5, pp. 712–724, 2014, doi. 10.1109/TCYB.2013.2279834.
[65] Z. Mokhtari and M. Sabbaghian, "Near-Optimal Angle of Transform in FrFT-OFDM Systems Based on ICI Analysis," IEEE Trans. Veh. Technol., vol. 65, no. 7, pp. 5777–5783, Jul. 2016, doi. 10.1109/TVT.2015.2460331.
[66] Xuezhong Wang, "Electronic radar signal recognition based on wavelet transform and convolution neural network," Alexandria Eng. J., vol. 61, no. 5, pp. 3559–3569, 2022, [Online]. Available.
https://www.sciencedirect.com/science/article/pii/S1110016821006049?via%3Dihub
[67] B. Ghahremani, M. Bitaraf, A. K. Ghorbani-Tanha, and R. Fallahi, "Structural damage identification based on fast S-transform and convolutional neural networks," Structures, vol. 29, pp. 1199–1209, 2021, [Online]. Available.
https://www.sciencedirect.com/science/article/abs/pii/S2352012420307104?via%3Dihub
[68] T. H. Thai and R. Cogranne, "Estimation of Primary Quantization Steps in Double-

Compressed JPEG Images Using a Statistical Model of Discrete Cosine Transform," IEEE Access, vol. 7, pp. 76203–76216, 2019, [Online]. Available. https://ieeexplore.ieee.org/document/8732320
[69] T. Y. Lee and H. W. Shen, "Efficient local statistical analysis via integral histograms with discrete wavelet transform," IEEE Trans. Vis. Comput. Graph., vol. 19, no. 12, pp. 2693–2702, 2013, doi. 10.1109/TVCG.2013.152.
[70] K. A. Rami Al-Hmouz, "License plate localization using a statistical analysis of Discrete Fourier Transform signal," Comput. Electr. Eng., vol. 40, no. 3, pp. 982–992, 2014, [Online]. Available.
https://www.sciencedirect.com/science/article/abs/pii/S004579061400007X?via%3Dihub
[71] W. P. Youhong Luo, Hui Liu, Chunye Wu, Maria Paraskevaidi c, Yujie Deng, Wenjie Shi, Ye Yuan, Ruifa Feng, Francis L. Martin, "Diagnostic segregation of human breast tumours using Fourier-transform infrared spectroscopy coupled with multivariate analysis. Classifying cancer subtypes," Spectrochim. Acta Part A Mol. Biomol. Spectrosc., vol. 255, p. 119694, 2021, [Online]. Available.
https://www.sciencedirect.com/science/article/abs/pii/S1386142521002705?via%3Dihub
[72] S. L. M. Jessica N. McCutcheon, Anthony R. Trimboli, Megan R. Pearl, Heather Brooke, Michael L. Myrick, "Diffuse reflectance infrared Fourier transform spectroscopy (DRIFTS) detection limits for blood on fabric. Orientation and coating uniformity effects," Sci. Justice, vol. 61, no. 5, pp. 603–616, 2021, doi. https://doi.org/10.1016/j.scijus.2021.07.003.
[73] K. R. Rao and N. Ahmed, "Orthogonal transforms for digital signal processing," ICASSP, IEEE Int. Conf. Acoust. Speech Signal Process. - Proc., vol. 1976-April, pp. 136–140, 1976, doi. 10.1109/ICASSP.1976.1170121.
[74] N. Ahmed and K. R. Rao, "Orthogonal Transforms for Digital Signal Processing," Orthogonal Transform. Digit. Signal Process., 1975, doi. 10.1007/978-3-642-45450-9.
[75] Y. A. Geadah and M. J. G. Corinthios, "Natural, Dyadic, and Sequency Order Algorithms and Processors for the Walsh-Hadamard Transform," IEEE Trans. Comput., vol. C–26, no. 5, pp. 435–442, 1977, doi. 10.1109/TC.1977.1674860.
[76] R. N. Boules, "Adaptive filtering using the fast Walsh-Hadamard transformation," IEEE Trans. Electromagn. Compat., vol. 31, no. 2, pp. 125–128, 1989, doi. 10.1109/15.18779.
[77] D. K. Rout, B. N. Subudhi, T. Veerakumar, and S. Chaudhury, "Walsh-Hadamard-Kernel-Based Features in Particle Filter Framework for Underwater Object Tracking," IEEE Trans. Ind. Informatics, vol. 16, no. 9, pp. 5712–5722, Sep. 2020, doi. 10.1109/TII.2019.2937902.
[78] A. Aung, "Sequency-ordered complex hadamard transforms and their applications to communications and signal processing," PhD, Sch. EEE, Nanyang Technol. Univ. Singapore, 2009, [Online]. Available. https://dr.ntu.edu.sg/handle/10356/18688
[79] A. Aung, B. P. Ng, and S. Rahardja, "Sequency-ordered complex Hadamard transform. Properties, computational complexity and applications," IEEE Trans. Signal Process., vol. 56, no. 8 I, pp. 3562–3571, Aug. 2008, doi. 10.1109/TSP.2008.923195.
[80] A. Aung and B. P. Ng, "Natural-ordered complex Hadamard transform," Signal Processing, vol. 90, no. 3, pp. 874–879, 2010, [Online]. Available. https://www.sciencedirect.com/science/article/abs/pii/S016516840900382X?via%3Dihub
[81] A. Aung, B. P. Ng, and S. Rahardja, "Conjugate symmetric sequency-ordered complex Hadamard transform," IEEE Trans. Signal Process., vol. 57, no. 7, pp. 2582–2593, 2009, doi. 10.1109/TSP.2009.2017572.
[82] F. Ohnsora, "spectral modes of the walsh-hadamard transform," IEEE Trans. Electromagn. Compat., vol. EMC-13, no. 3, pp. 55–59, 1971, doi. 10.1109/TEMC.1971.303109.
[83] H. X. Husheng Liu, Yinan Wang, Nan Li, "A Calibration Method for Nonlinear Mismatches in M-Channel Time-Interleaved Analog-to-Digital Converters Based on Hadamard Sequences," Appl. Sci., vol. 6, no. 11, p. 362, 2016, doi. https://doi.org/10.3390/app6110362.
[84] N. Ahmed, "Some considerations of the discrete Fourier and Walsh-Hadamard transforms," Proc. 1972 IEEE Conf. Decis. Control 11th Symp. Adapt. Process. New Orleans,

LA, USA, pp. 495–498, Apr. 2010, doi. 10.1109/CDC.1972.269054.
[85] A. L. Abdussattar, "On Cyclic Autocorrelation and the Waish-Hadamard Transform," IEEE Trans. Electromagn. Compat., vol. EMC-15, no. 3, pp. 141–146, 1973, doi. 10.1109/TEMC.1973.303280.
[86] K. J. Ray Liu, "A Simple and Unified Proof of Dyadic Shift Invariance and the Extension to Cyclic Shift Invariance," IEEE Trans. Educ., vol. 36, no. 4, pp. 369–372, 1993, doi. 10.1109/13.241613.
[87] K. Revuluri, K. R. Rao, M. A. Narasimhan, and N. Ahmed, "Cyclic and Dyadic Shifts, Walsh Hadamard Transform, and the H Diagram," IEEE Trans. Comput., vol. C–23, no. 12, pp. 1303–1306, 1974, doi. 10.1109/T-C.1974.223851.
[88] H. Hama and K. Yamashita, "Walsh-Hadamard Power Spectra Invariant to Certain Transform Groups," IEEE Trans. Syst. Man Cybern., vol. 9, no. 4, pp. 227–237, 1979, doi. 10.1109/TSMC.1979.4310184.
[89] W. D. Lyle and F. Forte, "A Useful Property of the Coefficients of a Walsh-Hadamard Transform," IEEE Trans. Acoust., vol. 28, no. 4, pp. 479–480, 1980, doi. 10.1109/TASSP.1980.1163434.
[90] S. Barnett, "Comment on 'A Useful Property of the Coefficients of a Walsh-Hadamard Transform,'" IEEE Trans. Acoust., vol. 29, no. 6, p. 1202, 1981, doi. 10.1109/TASSP.1981.1163690.
[91] C. Y. Hsu and J. L. Wu, "Block-diagonal structure of Walsh-Hadamard/discrete cosine transform," Electron. Lett., vol. 23, no. 21, pp. 1123–1124, 1987, doi. 10.1049/EL.19870783.
[92] B. J. Falkowski, "Properties and Ways of Calculation of Multi-Polarity Generalized Walsh Transforms," IEEE Trans. Circuits Syst. II Analog Digit. Signal Process., vol. 41, no. 6, pp. 380–391, 1994, doi. 10.1109/82.300195.
[93] S. R. Lee and M. H. Lee, "On the reverse jacket matrix for weighted hadamard transform," IEEE Trans. Circuits Syst. II Analog Digit. Signal Process., vol. 45, no. 3, pp. 436–441, 1998, doi. 10.1109/82.664258.
[94] E. W. Dorin Ervin Dutkay, John Haussermann, "Spectral properties of small Hadamard matrices," Linear Algebra Appl., vol. 506, pp. 363–381, 2016, doi. https.//doi.org/10.1016/j.laa.2016.06.006.
[95] D. O. Maria Carmela De Bonis, "Approximation of Hilbert and Hadamard transforms on (0,+∞)," Appl. Numer. Math., vol. 116, pp. 184–194, 2017, doi. https.//doi.org/10.1016/j.apnum.2016.12.001.
[96] S.-C. Pei, C.-C. Wen, and J.-J. Ding, "Sequency-ordered generalized Walsh–Fourier transform," Signal Processing, vol. 93, no. 4, pp. 828–841, 2013, [Online]. Available. https.//www.sciencedirect.com/science/article/abs/pii/S0165168412003660?via%3Dihub
[97] G. R. Redinbo, "An Implementation Technique for Walsh Functions," IEEE Trans. Comput., vol. C–20, no. 6, pp. 706–707, 1971, doi. 10.1109/T-C.1971.223332.
[98] D. Sundararajan and M. O. Ahmad, "Fast computation of the discrete Walsh and Hadamard transforms," IEEE Trans. Image Process., vol. 7, no. 6, pp. 898–904, 1998, doi. 10.1109/83.679439.
[99] H. C. Andrews, K. L. Caspari, and H. C. Andrews, "A Generalized Technique for Spectral Analysis," IEEE Trans. Comput., vol. C–19, no. 1, pp. 16–25, 1970, doi. 10.1109/TC.1970.5008895.
[100] M. Cohn and A. Lempel, "On Fast M-Sequence Transforms," IEEE Trans. Inf. Theory, vol. 23, no. 1, pp. 135–137, 1977, doi. 10.1109/TIT.1977.1055666.
[101] G. Bi and B. G. Evans, "Hardware structure for Walsh-Hadamard transforms," Electron. Lett., vol. 34, no. 21, pp. 2005–2006, Oct. 1998, doi. 10.1049/EL.19981425.
[102] D. Hein and N. Ahmed, "On a Real-Time Walsh-Hadamard/Cosine Transform Image Processor," IEEE Trans. Electromagn. Compat., vol. EMC-20, no. 3, pp. 453–457, 1978, doi. 10.1109/TEMC.1978.303679.
[103] J. L. Wu, "Block diagonal structure in discrete transforms," IEE Proc. E Comput. Digit.

Tech., vol. 136, no. 4, pp. 239–246, 1989, doi. 10.1049/IP-E.1989.0033;WEBSITE.WEBSITE.IET-SITE;WGROUP.STRING.PUBLICATION.
[104] J. Liang and T. D. Tran, "Fast multiplierless approximations of the DCT with the lifting scheme," IEEE Trans. Signal Process., vol. 49, no. 12, pp. 3032–3044, Dec. 2001, doi. 10.1109/78.969511.
[105] M. Masera, M. Martina, and G. Masera, "Adaptive Approximated DCT Architectures for HEVC," IEEE Trans. Circuits Syst. Video Technol., vol. 27, no. 12, pp. 2714–2725, Dec. 2017, doi. 10.1109/TCSVT.2016.2595320.
[106] P. Sharma, S. I. Ahson, and J. Henry, "Microprocessor Implementation of Fast Walsh-Hadamard Transform for Calculation of Symmetrical Components," Proc. IEEE, vol. 76, no. 10, pp. 1385–1388, 1988, doi. 10.1109/5.16340.
[107] S. Boussakta and A. G. J. Holt, "Fast algorithm for calculation of both Walsh-Hadamard and Fourier transforms (FWFTs)," Electron. Lett., vol. 25, no. 20, pp. 1352–1354, Sep. 1989, doi. 10.1049/EL.19890903.
[108] J. K. Pitas and A. N. Venetsanopoulos, "Two-Dimensional Realization of Digital Filters by Transform Decomposition," IEEE Trans. Circuits Syst., vol. 32, no. 10, pp. 1029–1040, 1985, doi. 10.1109/TCS.1985.1085623.
[109] J. S. Soundararajan and N. B. Chakraborti, "Performance of Adaptive Filters Using Combined Lattice and Transform Techniques," Proc. IEEE, vol. 74, no. 4, pp. 609–611, 1986, doi. 10.1109/PROC.1986.13511.
[110] G. Péceli and B. Fehér, "Digital Filters Based on Recursive Walsh-Hadamard Transformation," IEEE Trans. Circuits Syst., vol. 37, no. 1, pp. 150–152, 1990, doi. 10.1109/31.45706.
[111] A. Mahalanobis, S. Song, S. K. Mitra, and M. R. Petraglia, "Adaptive FIR Filters Based On Structural Subband Decomposition for System Identification Problems," IEEE Trans. Circuits Syst. II Analog Digit. Signal Process., vol. 40, no. 6, pp. 375–381, 1993, doi. 10.1109/82.277882.
[112] G. Deng, "Implementation of isotropic quadratic filters usingWalsh-Hadamard transform," Electron. Lett., vol. 31, no. 17, pp. 1422–1423, Aug. 1995, doi. 10.1049/EL.19950996.
[113] C. F. Chan, "Efficient implementation of class of isotropicquadratic filtersby using Walsh-Hadamard transform," Electron. Lett., vol. 35, no. 16, pp. 1306–1308, Aug. 1999, doi. 10.1049/EL.19990867.
[114] A. Amira, A. Bouridane, P. Milligan, and M. Roula, "Novel FPGA implementations of Walsh–Hadamard transforms for signal processing," IEE Proc. - Vision, Image Signal Process., vol. 148, no. 6, pp. 377–383, Dec. 2001, doi. 10.1049/IP-VIS.20010674.
[115] M. H. Lee, B. Sundar Rajan, and J. Y. Park, "A generalized reverse jacket transform," IEEE Trans. Circuits Syst. II Analog Digit. Signal Process., vol. 48, no. 7, pp. 684–690, Jul. 2001, doi. 10.1109/82.958338.
[116] M. S. Ahmed, S. Boussakta, B. S. Sharif, and C. C. Tsimenidis, "OFDM based on low complexity transform to increase multipath resilience and reduce PAPR," IEEE Trans. Signal Process., vol. 59, no. 12, pp. 5994–6007, Dec. 2011, doi. 10.1109/TSP.2011.2166551.
[117] S. H. Wang, C. P. Li, K. C. Lee, and H. J. Su, "A novel low-complexity precoded OFDM system with reduced PAPR," IEEE Trans. Signal Process., vol. 63, no. 6, pp. 1366–1376, Mar. 2015, doi. 10.1109/TSP.2015.2389751.
[118] C. Kang, Y. Liu, M. Hu, and H. Zhang, "A low complexity PAPR reduction method based on FWFT and PEC for OFDM systems," IEEE Trans. Broadcast., vol. 63, no. 2, pp. 416–425, Jun. 2017, doi. 10.1109/TBC.2016.2637278.
[119] A. Khan, A. Arif, T. Nawaz, and S. Baig, "Walsh Hadamard transform based transceiver design for SC-FDMA with discrete wavelet transform," China Commun., vol. 14, no. 5, pp. 193–206, May 2017, doi. 10.1109/CC.2017.7942326.
[120] M. T. Hamood and S. Boussakta, "Fast Walsh–Hadamard–Fourier Transform Algorithm," IEEE Trans. Signal Process., vol. 59, no. 11, pp. 5627–5631, 2011, [Online].

Available. https://ieeexplore.ieee.org/document/5960801
[121] E. and Y. B. Tisserand, "Original structure for Walsh-Hadamard transform on sliding window," Electron. Lett., vol. 51, no. 23, pp. 1850–1852, 2015, [Online]. Available. https://ietresearch.onlinelibrary.wiley.com/doi/epdf/10.1049/el.2015.1246
[122] B. Singer and M. M. Veloso, "Automating the modeling and optimization of the performance of signal transforms," IEEE Trans. Signal Process., vol. 50, no. 8, pp. 2003–2014, Aug. 2002, doi. 10.1109/TSP.2002.800394.
[123] S. Bouguezel, M. O. Ahmad, and M. N. S. Swamy, "Binary discrete cosine and hartley transforms," IEEE Trans. Circuits Syst. I Regul. Pap., vol. 60, no. 4, pp. 989–1002, 2013, doi. 10.1109/TCSI.2012.2224751.
[124] S. H. and M. V. R. Scheibler, "A Fast Hadamard Transform for Signals With Sublinear Sparsity in the Transform Domain," IEEE Trans. Inf. Theory, vol. 61, no. 4, pp. 2115–2132, 2015, [Online]. Available. https://ieeexplore.ieee.org/document/7042831
[125] N. Park and V. K. Prasanna, "Dynamic data layouts for cache-conscious implementation of a class of signal transforms," IEEE Trans. Signal Process., vol. 52, no. 7, pp. 2120–2134, Jul. 2004, doi. 10.1109/TSP.2004.828946.
[126] A. Thompson, "The cascading haar wavelet algorithm for computing the Walsh-Hadamard transform," IEEE Signal Process. Lett., vol. 24, no. 7, pp. 1020–1023, Jul. 2017, doi. 10.1109/LSP.2017.2705247.
[127] P. Marti-Puig, "A family of fast Walsh Hadamard algorithms with identical sparse matrix factorization," IEEE Signal Process. Lett., vol. 13, no. 11, pp. 672–675, Nov. 2006, doi. 10.1109/LSP.2006.879472.
[128] A. Iossifides and S. Louvros, "A new aspect of walsh-hadamard coding over rayleigh fading channels," IEEE Lat. Am. Trans., vol. 10, no. 3, pp. 1680–1685, 2012, doi. 10.1109/TLA.2012.6222570.
[129] O. U. Khan, S. Y. Chen, D. D. Wentzloff, and W. E. Stark, "Impact of compressed sensing with quantization on UWB receivers with multipath channel estimation," IEEE J. Emerg. Sel. Top. Circuits Syst., vol. 2, no. 3, pp. 460–469, 2012, doi. 10.1109/JETCAS.2012.2222220.
[130] N. Michailow, L. Mendes, M. Matthe, I. Gaspar, A. Festag, and G. Fettweis, "Robust WHT-GFDM for the next generation of wireless networks," IEEE Commun. Lett., vol. 19, no. 1, pp. 106–109, Jan. 2015, doi. 10.1109/LCOMM.2014.2374181.
[131] H. W. Jones, "A Comparison of Theoretical and Experimental Video Compression Designs," IEEE Trans. Electromagn. Compat., vol. EMC-21, no. 1, pp. 50–56, 1979, doi. 10.1109/TEMC.1979.303797.
[132] et al Pauchard, Y., "Fast computation of residual complexity image similarity metric using low-complexity transforms," IET Image Process., vol. 9, no. 8, pp. 699–708, 2015, [Online]. Available. https://ietresearch.onlinelibrary.wiley.com/doi/epdf/10.1049/iet-ipr.2014.0939
[133] P. . Mali, B. . Chaudhuri, and D. D. Majumder, "Performance bound of Walsh-Hadamard transform for feature selection and compression and some related fast algorithms," Pattern Recognit. Lett., vol. 2, no. 1, pp. 5–12, 1983, doi. https://doi.org/10.1016/0167-8655(83)90015-6.
[134] T.-Y. C. Ho-Youl Jung, Rémy Prost, "A unified mathematical form of the Walsh-Hadamard transform for lossless image data compression," Signal Processing, vol. 63, no. 1, pp. 35–43, 1997, doi. https://doi.org/10.1016/S0165-1684(97)00138-2.
[135] and B. w. k. L. Ou, G.w., D.p.k. Lun, "Compressive sensing of images based on discrete periodic radon transform," Electron. Lett., vol. 50, no. 8, pp. 591–593, 2014, [Online]. Available. https://ietresearch.onlinelibrary.wiley.com/doi/epdf/10.1049/el.2014.0770
[136] Z. Lian and M. J. Er, "Illumination normalisation for face recognition in transformed domain," Electron. Lett., vol. 46, no. 15, pp. 1060–1061, Jul. 2010, doi. 10.1049/EL.2010.1495.
[137] E. S. McVey and R. M. Inigo, "A Multilayered Self-Organizing Artificial Neural Network for Invariant Pattern Recognition," IEEE Trans. Knowl. Data Eng., vol. 4, no. 2, pp. 162–167, 1992, doi. 10.1109/69.134253.

[138] M. K. K. Santi P. Maity, "Perceptually adaptive spread transform image watermarking scheme using Hadamard transform," Inf. Sci. (Ny)., vol. 181, no. 3, pp. 450–465, 2011, doi. https://doi.org/10.1016/j.ins.2010.09.029.
[139] Y. Ishikawa, K. Uehira, and K. Yanaka, "Optimization of size of pixel blocks for orthogonal transform in optical watermarking technique," IEEE/OSA J. Disp. Technol., vol. 8, no. 9, pp. 505–510, 2012, doi. 10.1109/JDT.2012.2201133.
[140] S. Z. Le Wang, Li Zou, "Edge detection based on subpixel-speckle-shifting ghost imaging," Opt. Commun., vol. 407, pp. 181–185, 2018, doi. https://doi.org/10.1016/j.optcom.2017.09.002.
[141] A. E. and W. B. F. Shum, "Speech processing with Walsh-Hadamard transforms," IEEE Trans. Audio Electroacoust., vol. 21, no. 3, pp. 174–179, 1973, doi. 10.1109/TAU.1973.1162475.
[142] J. Pearl, "Application of Walsh Transform to Statistical Analysis," IEEE Trans. Syst. Man. Cybern., vol. 1, no. 2, pp. 111–119, 1971, [Online]. Available. https://ieeexplore.ieee.org/document/4308267
[143] P. Yip and K. Rao, "Energy Packing Efficiency for the Generalized Discrete Transforms," IEEE Trans. Commun., vol. 26, no. 8, pp. 1257–1262, 1978, doi. 10.1109/TCOM.1978.1094199.
[144] H. Burkhardt and X. Muller, "On invariant sets of a certain class of fast translation-invariant transforms," IEEE Trans. Acoust., vol. 28, no. 5, pp. 517–523, 1980, [Online]. Available. https://ieeexplore.ieee.org/document/1163439
[145] B. Arambepola and K.C. Partington, "Walsh-Hadamard transform for complex-valued signals," Electron. Lett., vol. 28, no. 3, 1992, doi. https://doi.org/10.1049/el.19920160.
[146] L. and Z. P. Dong, "Fast motion estimation algorithm using multilevel distortion search in Walsh-Hadamard domain," IET Image Process., vol. 11, no. 1, pp. 22–30, 2017, [Online]. Available. https://ietresearch.onlinelibrary.wiley.com/doi/epdf/10.1049/iet-ipr.2016.0453
[147] P. W. Besslich, "Determination of the irredundant forms of a Boolean function using Walsh-Hadamard analysis and dyadic groups," IEE J. Comput. Digit. Tech., vol. 1, no. 4, pp. 143–151, 1978, doi. 10.1049/IJ-CDT.1978.0041.
[148] N. Ahmed and K. Rao, "Additional properties of complex BIFORE transform," IEEE Trans. Audio Electroacoust., vol. 19, no. 3, pp. 252–253, 1971, doi. 10.1109/TAU.1971.1162190.
[149] S. Rahardja and B. J. Falkowski, "Family of unified complex Hadamard transforms," IEEE Trans. Circuits Syst. II Analog Digit. Signal Process., vol. 46, no. 8, pp. 1094–1100, 1999, [Online]. Available. https://ieeexplore.ieee.org/document/782059
[150] S. Rahardja and B. J. Falkowski, "Family of complex Hadamard transforms. relationship with other transforms and complex composite spectra," Proc. Int. Symp. Mult. Log., pp. 125–130, 1997, doi. 10.1109/ISMVL.1997.601386.
[151] B. J. Falkowski and S. Rahardja, "Properties and applications of unified complex Hadamard transforms," Proc. Int. Symp. Mult. Log., pp. 131–136, 1997, doi. 10.1109/ISMVL.1997.601387.
[152] B. J. Falkowski, "Family of generalised multi-polaritycomplex Hadamard transforms," IEE Proc. - Vision, Image Signal Process., vol. 145, no. 6, pp. 371–378, Dec. 1998, doi. 10.1049/IP-VIS.19982461.
[153] S. Rahardja and B. J. Falkowski, "Complex composite spectra of Unified Complex Hadamard transform for logic functions," IEEE Trans. Circuits Syst. II Analog Digit. Signal Process., vol. 47, no. 11, pp. 1291–1296, Nov. 2000, doi. 10.1109/82.885135.
[154] S. Rahardja, W. Ser, and Z. Lin, "UCHT-based complex sequences for asynchronous CDMA system," IEEE Trans. Commun., vol. 51, no. 4, pp. 618–626, Apr. 2003, doi. 10.1109/TCOMM.2003.810798.
[155] S. Xie and S. Rahardja, "Performance evaluation for quaternary DS-SSMA communications with complex signature sequences over Rayleigh-fading channels," IEEE Trans. Wirel. Commun., vol. 4, no. 1, pp. 266–277, Jan. 2005, doi. 10.1109/TWC.2004.840203.
[156] S. Xie, S. Rahardja, and Z. Gu, "Performance of DS-CDMA downlink systems with orthogonal UCHT complex sequences," IEEE Trans. Commun., vol. 55, no. 2, pp. 251–256, 2007,

doi. 10.1109/TCOMM.2006.888524.
[157] A. Aung, B. P. Ng, and S. Rahardja, "Performance of SCHT sequences in asynchronous CDMA system," IEEE Commun. Lett., vol. 11, no. 8, pp. 641–643, Aug. 2007, doi. 10.1109/LCOMM.2007.070407.
[158] G. Bi, A. Aung, and B. Poh Ng, "Pipelined hardware structure for sequency-ordered complex hadamard transform," IEEE Signal Process. Lett., vol. 15, pp. 401–404, 2008, doi. 10.1109/LSP.2008.922515.
[159] A. Aung, B. P. Ng, and S. Rahardja, "A robust watermarking scheme using sequency-ordered complex hadamard transform," J. Signal Process. Syst., vol. 64, no. 3, pp. 319–333, May 2011, doi. 10.1007/S11265-010-0492-7/METRICS.
[160] J. Wu, H. Shu, L. Wang, and L. Senhadji, "Fast algorithms for the computation of sliding sequency-ordered complex hadamard transform," IEEE Trans. Signal Process., vol. 58, no. 11, pp. 5901–5909, 2010, doi. 10.1109/TSP.2010.2063026.
[161] N. Swetha, P. N. Sastry, Y. R. Rao, and S. L. Sabat, "Fast Sequency-Ordered Complex Hadamard Transform-Based Parzen Window Entropy Detection for Spectrum Sensing in Cognitive Radio Networks," IEEE Commun. Lett., vol. 20, no. 7, pp. 1401–1404, Jul. 2016, doi. 10.1109/LCOMM.2016.2548466.
[162] V. S. Padmavathi Kora, Ambika Annavarapu, Priyanka Yadlapalli, K. Sri Rama Krishna, "ECG based Atrial Fibrillation detection using Sequency Ordered Complex Hadamard Transform and Hybrid Firefly Algorithm," Eng. Sci. Technol. an Int. J., vol. 20, no. 3, pp. 1084–1091, 2017, [Online]. Available. https.//www.sciencedirect.com/science/article/pii/S221509861630684X
[163] L. S. and H. S. J. Wu, L. Wang, "Sliding conjugate symmetric sequency-ordered complex hadamard transform. Fast algorithm and applications," 2010 18th Eur. Signal Process. Conf. Aalborg, Denmark, pp. 1742–1746, 2010, [Online]. Available. https.//ieeexplore.ieee.org/document/7096450
[164] S. C. Pei, C. C. Wen, and J. J. Ding, "Conjugate symmetric discrete orthogonal transform," IEEE Trans. Circuits Syst. II Express Briefs, vol. 61, no. 4, pp. 284–288, 2014, doi. 10.1109/TCSII.2014.2305011.
[165] S. Kyochi and Y. Tanaka, "General Factorization of Conjugate-Symmetric Hadamard Transforms," IEEE Trans. Signal Process., vol. 62, no. 13, pp. 3379–3392, 2014, [Online]. Available. https.//ieeexplore.ieee.org/document/6820782
[166] D. Jabeen, G. Monir, and F. Azim, "Sequency Domain Signal Processing Using Complex Hadamard Transform," Circuits, Syst. Signal Process., vol. 35, no. 5, pp. 1783–1793, May 2016, doi. 10.1007/S00034-015-0138-X/METRICS.
[167] D. and G. M. Jabeen, "Two-dimensional spatiochromatic signal processing using concept of phasors in sequency domain," Electron. Lett., vol. 52, no. 11, pp. 968–970, 2016, [Online]. Available. https.//ietresearch.onlinelibrary.wiley.com/doi/epdf/10.1049/el.2016.0059
[168] M. F. K. Dure Jabeen, T.I., "Multidimensional signal processing using quaternion complex Hadamard transform in sequency domain," Electron. Lett., vol. 54, no. 25, pp. 1435–1436, 2018, [Online]. Available. https.//ietresearch.onlinelibrary.wiley.com/doi/epdf/10.1049/el.2018.6548
[169] J. Wu et al, "Fast Gray Code Kernel Algorithm for the Sliding Conjugate Symmetric Sequency-Ordered Complex Hadamard Transform," IEEE Access, vol. 6, pp. 56029–56045, 2018, doi. 10.1109/ACCESS.2018.2871885.
[170] D. Jabeen, S. M. G. Monir, S. Noor, M. Rafiullah, and M. A. Jatoi, "Color image watermarking using spatio-chromatic complex Hadamard transform in sequency domain," World J. Eng., vol. 19, no. 5, pp. 658–666, Aug. 2022, doi. 10.1108/WJE-03-2021-0176/FULL/XML.
[171] C. H. C. Heng, I., "Error correcting codes associated with complex Hadamard matrices," Appl. Math. Lett., vol. 11, no. 4, pp. 77–80, 1998, doi. https.//doi.org/10.1016/S0893-9659(98)00059-7.
[172] S. Rahardja and B. J. Falkowski, "Symmetry conditions of Boolean functions incomplex Hadamard transform," Electron. Lett., vol. 34, no. 17, pp. 1634–1635, Aug. 1998, doi. 10.1049/EL.19981164.

[173] L. L. Bin Wang , Jiasong Wu, Huazhong Shu, "Shape description using sequency-ordered complex Hadamard transform," Opt. Commun., vol. 284, no. 12, pp. 2726–2729, 2011, doi. https://doi.org/10.1016/j.optcom.2011.01.061.
[174] P. R. J. Ö. Pekka H.J. Lampio, Ferenc Szöllősi, "The quaternary complex Hadamard matrices of orders 10, 12, and 14," Discrete Math., vol. 313, no. 2, pp. 189–206, 2013, [Online]. Available. https://www.sciencedirect.com/science/article/pii/S0012365X12004384
[175] J. Liu, Q. Xing, X. Yin, X. Mao, and F. Yu, "Pipelined Architecture for a Radix-2 Fast Walsh-Hadamard-Fourier Transform Algorithm," IEEE Trans. Circuits Syst. II Express Briefs, vol. 62, no. 11, pp. 1083–1087, Nov. 2015, doi. 10.1109/TCSII.2015.2456371.
[176] Bengt R. Karlsson, "Three-parameter complex Hadamard matrices of order 6," Linear Algebra Appl., vol. 434, pp. 247–258, 2011, doi. https://doi.org/10.1016/j.laa.2010.08.020.
[177] K. Meenakshi, K. Satya Prasad, and C. Srinivasa Rao, "Development of Low-Complexity Video Watermarking with Conjugate Symmetric Sequency-Complex Hadamard Transform," IEEE Commun. Lett., vol. 21, no. 8, pp. 1779–1782, Aug. 2017, doi. 10.1109/LCOMM.2017.2700461.
[178] M. H. L. and Y. J. H. Hai, X. -Q. Jiang, W. Duan, J. Li, "Complex Hadamard Matrix-Aided Generalized Space Shift Keying Modulation," IEEE Access, vol. 5, pp. 21139–21147, 2017, doi. 10.1109/ACCESS.2017.2758269.
[179] Ferenc Szöllősi, "Parametrizing complex Hadamard matrices," Eur. J. Comb., vol. 29, no. 5, pp. 1219–1234, 2008, doi. https://doi.org/10.1016/j.ejc.2007.06.009.
[180] Ferenc Szöllősi, "Complex Hadamard matrices and equiangular tight frames," Linear Algebra Appl., vol. 438, no. 4, pp. 1962–1967, 2013, doi. https://doi.org/10.1016/j.laa.2011.05.034.
[181] J.-M. S. Gaurush Hiranandani, "Small circulant complex Hadamard matrices of Butson type," Eur. J. Comb., vol. 51, pp. 306–314, 2016, doi. https://doi.org/10.1016/j.ejc.2015.05.010.
[182] Z.-C. Fan, D. Li, and S. Rahardja, "Efficient Computation for Discrete Fractional Hadamard Transform," IEEE Trans. Circuits Syst. I Regul. Pap., pp. 1–9, Aug. 2024, doi. 10.1109/TCSI.2024.3441834.
[183] R. Bomfin and M. Chafii, "Sparse-DFT and WHT Precoding with Iterative Detection for Highly Frequency-Selective Channels," IEEE Trans. Wirel. Commun., vol. 23, no. 5, pp. 4083–4096, May 2024, doi. 10.1109/TWC.2023.3314075.
[184] H. Pan, E. Hamdan, X. Zhu, S. Atici, and A. E. Cetin, "Multichannel Orthogonal Transform-Based Perceptron Layers for Efficient ResNets," IEEE Trans. Neural Networks Learn. Syst., 2024, doi. 10.1109/TNNLS.2024.3384316.